Utilisation d'un Mécanisme Parallèle à Faible Impédance pour une Interaction Humain-Robot Intuitive et Hautement Réactive

Mémoire

Gabriel Boucher

Maîtrise en génie mécanique - avec mémoire
Maître ès sciences (M. Sc.)

Québec, Canada

Résumé

Ce mémoire présente la conception d'un mécanisme parallèle passif élastique utilisé afin de contrôler un robot sériel à 5 degrés de liberté de façon sécuritaire et intuitive. Ce mémoire présente deux articles qui ont été écrits dans le cadre du projet et qui présentent dans un premier temps l'algorithme de contrôle sur lequel le concept est basé, et dans un deuxième temps le prototype du mécanisme passif servant à détecter les mouvements.

L'algorithme de contrôle est inspiré par le concept de manipulateur macro/mini où l'utilisateur interagit avec un mécanisme passif à faible impédance afin de contrôler le mouvement d'un mécanisme actionné qui a une plus grande impédance. Le concept, déjà utilisé pour des manipulateurs de type portique, est étendu à un robot sériel à plusieurs degrés de liberté. L'algorithme utilise une mesure de déplacement du mini-manipulateur passif afin d'appliquer des couples aux moteurs du macro-mainpulateur actionné. Afin de détecter les déplacements, un capteur à 6 degrés de liberté est conçu. L'architecture du capteur, qui est basée sur la platforme de Gough-Stewart, consiste en un mécanisme parallèle assemblé sur une membrure du robot sériel. Des résultats expérimentaux sont présentés.

Abstract

This thesis presents the design and experimental validation of a passive elastic parallel mechanism used to control intuitively and safely a five-degree-of-freedom serial robot. The thesis presents two articles which were written in the course of the project. The articles present, firstly, the control algorithm which is the basis of the concept, and secondly, the mechanical design of the passive mechanism.

The algorithm is inspired from the macro/mini architecture where the human user interacts with a low-impedance passive mechanism in order to control the motion of a larger actuated mechanism which has a higher impedance. This concept, used on gantry manipulators, is extended to a serial robot with multiple degrees of freedom. The algorithm uses a displacement measurement from the passive mechanism in order to compute and apply torques to the actuated mechanism. In order to measure the displacements, a passive six-degree-of-freedom mechanism is designed. The architecture of the sensor, based on the Gough-Stewart platform, is in fact a passive parallel mechanism mounted around the link of a serial robot. Experimental results are provided.

Table des matières

Liste des figures

À mes parents

Hell... it's about time

Tychus Findlay

Remerciements

Dès mon entrée à l'université, j'avais comme but de compléter une maîtrise dans un domaine qui m'intéressait, mais je n'avais aucune idée que ce domaine serait celui de la robotique.

Premièrement, je tiens à remercier mon directeur de recherche, Clément Gosselin. Merci de m'avoir tout d'abord offert la chance de faire un stage qui m'a fait découvrir le monde facinant de la robotique. Bien que je ne sache pas comment il fait, Clément est toujours présent pour les étudiants afin d'encadrer la recherche d'une manière exceptionnelle. Au-delà de sa maîtrise exceptionnelle du sujet, sa capacité à superviser et enseigner en fait un directeur hors pair. Merci pour tout.

Ensuite, merci au membres du laboratoire de robotique. Merci surtout à Thierry et Simon pour leur aide précieuse lors du développement du prototype. Thierry pour ses conceils lors de la conception mécanique et Simon pour les heures passées à faire fonctionner la communication et *Simulink Real Time*. Merci à tous pour les parties de badminton, de spikeball, et de soccer.

Finalement, merci à mes parents. Leur support tout au long de mes longues études est inestimable et je ne leur dirai jamais assez merci pour m'avoir permis de poursuivre des études graduées. Je n'y serais sans doute jamais arrivé sans leur support. Merci.

Avant-propos

Le mémoire présenté est écrit sous la forme d'un mémoire par articles. Différentes informations doivent tout d'abord être présentées soit : le statut des articles en date de soumission du mémoire, les modifications aux articles s'il y a lieu, mon statut d'auteur ainsi que celui des co-auteurs s'il y a lieu, et finalement mon rôle exact dans la préparation des articles. Ces informations sont données en point de forme pour chaque article par souci d'efficacité.

Chapitre 1

Titre : A parallel low-impedance sensing approach for highly responsive physical human-robot interaction

Type d'article : Article de conférence, ICRA 2019

Statut : Article accepté à la conférence ICRA 2019.

Contribution : Auteur principal. Écriture, conception du mécanisme, du bras robotique, et de l'algorithme de contrôle, ainsi que l'expérimentation faits par l'auteur principal.

Coauteurs : Prof. Clément Gosselin a supervisé les travaux et révisé l'article afin d'assurer la finalité de celui-ci. Thierry Laliberté a participé activement à la conception du bras robotique utilisé pour les tests et à la conception des vérins utilisés dans le mécanisme.

Modification : Aucune modification. Le chapitre correspond à la version finale de l'article soumise à la conférence.

Chapitre 2

Titre : Mechanical design and experimental validation of a low-impedance 6-degree-of-freedom displacement sensor for intuitive physical human-robot interaction

Type d'article : Article de Journal

Statut : Non-soumis. Version de l'article prête à être soumise.

Contribution : Auteur principal. Écriture, conception de l'architecture et de la structure du mécanisme, ainsi que le développement de la cinématique et statique de celui-ci ont été effectués par l'auteur principal. L'expérimentation fut aussi réalisée par ce dernier.

Coauteurs : Prof. Clément Gosselin a supervisé les travaux et révisé l'article afin d'assurer la finalité de celui-ci. Thierry Laliberté a participé activement à la conception du bras robotique utilisé pour les tests et la conception des vérins utilisés dans le mécanisme ainsi que la révision d'une partie de l'article.

Modification : Aucune modification apportée pour l'instant.

Introduction

Depuis plusieurs années déjà, l'automatisation ainsi que les robots prennent de plus en plus de place dans notre société. Que ce soit dans l'industrie manufacturière ou bien à la maison, les robots sont utilisés pour une très grande variété de tâches. Un des exemples les plus classiques de robots est bien entendu ceux que l'on peut apercevoir dans les usines et sur les chaines de montage. Ces robots sont généralement utilisés afin de remplacer des humains dans des tâches qui sont répétitives, exténuantes ou bien dangereuses. Ces robots sont souvent isolés et ne travaillent pas dans le même environement que les humains. Ils sont très puissants et rapides, ce qui est un avantage pour la production de masse, mais requiert beaucoup de dispositifs externes afin d'être sécuritaires. De plus, ces robots sont souvent relativement complexes à programmer car ils ne sont pas nécessairement intuitifs.

De nos jours, les robots ont aussi commencé à faire leur apparition dans les maisons. Un exemple populaire est les divers robots aspirateurs utilisés pour faire le ménage. Par contre, ces robots sont des robots mobiles et sont bien loins des robots industriels mentionnés plus haut. Ces robots sont souvent lents et peu puissants. Ils ne sont pas dangereux et ne requièrent pas de système de sécurité.

Tout récement, une nouvelle gamme de robots a fait son entrée sur le marché : les robots collaboratifs. Ces robots sont généralement des bras robotques sériels, similaires à ceux utilisés dans les applications industrielles. Par contre, ces robots diffèrent des robots industriels en deux points. Premièrement, ces robots sont moins puissants que les robots industriels. La charge utile est généralement limitée à quelques kilogrammes et la vitesse des articulations et de l'effecteur sont grandement limitées. Par contre, ces deux facteurs font en sorte que les robots collaboratifs sont beaucoup plus sécuritaires que les robots industriels et peuvent donc être utilisés dans le même espace que des humains. Bien que leurs performances soient moins bonnes que celles des robots industriels, ces robots sont idéals pour simplifier certaines tâches où la vitesse et la force ne sont pas nécessaires. Les robots collaboratifs performent particulièrement bien dans des tâches comme l'assemblage simple, les applications de *pick-and-place*, ou bien le chargement et déchargement de pièces dans les machines-outils. De plus, des performances limitées et une plus grande sécurité permettent de réduire le coût des robots collaboratifs eux-mêmes, ainsi que d'économiser en n'ayant pas besoin d'installer des systèmes de sécurité. Ces robots sont donc de plus en plus utilisés par de plus petites entreprises qui n'ont peut-être pas l'expertise pour opérer des systèmes robotisés complexes. Il faut donc que ces robots deviennent non seulement de plus en plus sécuritaires, mais aussi de plus en plus simples à opérer. L'interaction

entre l'opérateur humain et le robot devient donc très importante.

La question de l'interaction entre les robots et les humains est encore très ouverte, autant au niveau de la sécurité des robots collaboratifs que des méthodes utilisées afin de rendre l'expérience intuitive et simple pour l'utilisateur. Des normes existent afin de rendre les robots collaboratifs sécuritaires, mais elles se résument souvent à les rendre lents et peu puissants. La détection de collision est souvent employée afin de limiter la force des robots et de les rendre plus sécuritaires.

L'autre volet de la collaboration humain-robot porte sur les méthodes d'interaction. Comme mentionné plus haut, ces robots sont souvent utilisés par des opérateurs ayant peu d'expérience ou de connaissances en robotique. Il faut donc que les robots soient simples à utiliser et que les efforts déployés par les opérateurs soient minimaux. Si le système est trop complexe ou fatiguant, l'opérateur peut perdre beaucoup de temps lors de l'éxecution d'une tâche. Le projet présenté dans ce mémoire porte principalement sur le volet de la méthode d'interaction.

Problématique

Méthode de contrôle

Traditionellement, les robots sont utilisés afin d'accomplir des tâches automatiquement sans la présence d'un utilisateur humain. Les méthodes de contrôle utilisées lors de l'accomplissement de ces tâches peuvent parfois prendre en compte certains capteurs externes afin de détecter des collisions, mais la tâche comme telle est souvent programmée d'avance. En robotique collaborative, on cherche soit à compléter une tâche sans avoir à programmer une trajectoire à l'avance, ou bien à simplifier la programmation en déplaçant le robot aux points d'intérêt facilement. Plus simplement, on cherche à deviner l'intention de l'utilisateur afin de déplacer le robot dans la direction voulue.

Certaines solutions existent déjà afin d'accomplir cette tâche. Certains robots utilisent une interface avec des boutons ou *joysticks* afin que l'utilisateur puisse diriger le robot dans la direction voulue. Cette méthode, bien que simple, est très peu intuitive car l'utilisateur doit avoir une bonne connaissance du repère utilisé et de la position du robot afin de l'utiliser.

D'autres méthodes, comme le contrôle par impédance ou admittance, nécessitent un contact direct avec le robot. Lorsqu'on contrôle un robot par impédance ou admittance, on mesure un déplacement ou bien une force afin de déduire l'intention de l'utilisateur. Ces méthodes sont très intuitives car l'interaction avec le robot est directe et aucune connaissance du robot ou du repère n'est nécessaire. Par contre, la nécessité d'un contact avec le robot amène deux points négatifs. Tout d'abord, en cas de collision, l'inertie du robot au complet sera ressentie par l'utilisateur et même avec une détection de collision adéquate, il n'y a pas de marge de manoeuvre lors d'une collision. Ensuite, lors de l'interaction avec le robot, l'utilisateur doit imposer une force qui fera déplacer l'ensemble du robot. Cela à pour effet de rendre l'interaction moins agréable et plus fatigante pour l'utilisateur qui doit combattre l'inertie du robot lors des accélérations.

Le principe de manipulateur macro/mini est une autre méthode de contrôle qui permet un contrôle intuitif et simple sans avoir à interagir directement avec le manipulateur. En effet, cette méthode utilise un mécanisme élastique passif comme interface avec laquelle l'utilisateur interagit afin de contrôler le mécanisme actif. Cette méthode, qui est une forme de contrôle par impédance, combine l'intuitivité du contrôle par impédance sans les inconvénients du contact direct avec le manipulateur. Cette approche est déjà utilisée pour des robots de type portique découplés en translation. Pour ces types de robots, le mécanisme passif supporte aussi la charge transportée. Afin d'utiliser cette méthode sur un robot sériel qui change d'orientation, certaines modifications doivent être apportées au concept. Entre autres, la charge doit être supportée par le mécanisme actif au lieu du mécanisme passif et l'algorithme de contrôle doit transformer les mouvements cartésiens en mouvements articulaires. Le mécanisme passif doit aussi être résistant aux changements d'orientations.

L'algorithme de contrôle doit aussi être assez performant et robuste, et ce même lors de mouvements rapides et oscillatoires.

Détection de mouvements

La détection de mouvements en robotique est un aspect important dans la plupart des applications. Pour les robot mobiles on peut chercher à savoir la position précise du robot dans l'espace. Pour les robots statiques plus traditionnels, on veut connaître la position de l'effecteur afin d'effectuer diverses tâches. La détection de mouvement prend un autre sens lors de la collabration entre un humain et un robot. En effet, les mouvements que l'on souhaite connaître ne sont pas seulement ceux du robot, mais aussi ceux de l'utilisateur. En effet, les mouvements de l'utilisateur servent ensuite à déduire l'intention de ce dernier et ces mouvements sont ensuite utilisés afin de contrôler le robot.

Les diverses approches de collaboration humain-robot utilisent presque toutes une mesure de mouvement quelconque. Le contrôle par impédance classique utilise directement le mouvement des encodeurs du robot afin d'évaluer l'intention de l'utilisateur. Le contrôle en force se sert d'une mesure de force afin de bouger le robot. Par contre, une mesure de force directe n'est pas physiquement possible, et les capteurs de force sont en effet des capteurs de mouvement à une échelle si petite que l'utilisateur ne le ressent pas. L'approche macro/mini utilise une interface passive afin de mesurer les mouvements de l'effecteur du robot. Cette méthode de détection de mouvement s'apparente beaucoup à la méthode par impédance, car une mesure est faite aux articulations d'un manipulateur, la différence étant que ce ne sont pas les articulations du manipulateur actif. Cette approche comporte certains avantages notamment la possibilité de détecter des mouvements à une échelle beaucoup plus grande que les autres méthodes.

Projet de recherche

La collaboration intuitive entre un utilisateur humain et un bras robotique est l'objet général du projet de maîtrise présenté dans ce mémoire. Le projet se veut une preuve de concept pour un système

de contrôle inspiré de l'architecture macro/mini utilisée pour des manipulateurs de type portique. Le projet peut être séparé en deux section. La première consiste à étendre le principe du système actif/passif à 1 degré de liberté vers une version générale applicable à un robot sériel à plusieurs degrés de liberté. Cette méthode doit donc prendre en compte des déplacements mesurés dans plusieurs axes ainsi qu'un nombre quelconque d'actionneurs. Ensuite, un schéma de commande par impédance est développé afin de contrôler un bras robotique à l'aide d'un capteur de déplacement passif élastique. Le deuxième volet du projet consiste à concevoir et fabriquer un capteur de mouvement passif pouvant mesurer 3 translations et 3 rotations. Le capteur doit aussi être mécaniquement intégré à un bras robotique. Plus précisément, le capteur doit être installé autour d'une des membrures du bras robotique sans nuire aux mouvements du robot.

Le robot en question est un bras robotique conçu et fabriqué au Laboratoire de Robotique. Le design est prévu pour accommoder le mécanisme du capteur de mouvement ainsi que la coquille mobile.

Plan du mémoire et méthodologie de recherche

Plan du mémoire

Comme mentionné dans l'avant-propos de ce mémoire, les chapitres sont écrits sous forme d'articles scientifiques. La problématique peut être séparée en deux points distincts soit : la méthode de contrôle et la détection de mouvement. Bien que ces deux points furent plus ou mois approchés simultanément lors de l'accomplissement du projet, l'écriture des articles reflète bien les deux aspects de la problématique. Le premier article (Chapitre 1) porte principalement sur la méthode de contrôle générale. Bien que l'article mentionne le capteur de mouvement utilisé pour l'expérimentation, ce dernier n'est pas exploré en profondeur. Le deuxième article (Chapitre 2) quant à lui porte entièrement sur la conception mécanique du capteur de mouvements. Encore une fois, une allusion est faite à la méthode de contrôle mais aucun détail n'est donné. Les deux chapitres peuvent se lire individuellement sans connaissance de l'autre mais sont tout de même cohérents dans l'ensemble du projet qui est, au final, la conception d'un robot sériel collaboratif. Un détail important à noter est que la méthode de contrôle est présentée avant la détection de mouvement même si la détection de mouvement fait partie intégrante de l'algorithme de contrôle. Ce choix est fait car la méthode de contrôle sert de contexte à la conception du capteur de mouvement présenté.

Méthodologie de recherche

Puisque les différents chapitres sont constitués d'articles scientifiques, la méthodologie utilisée n'est pas explicitement décrites dans les chapitres. Les articles ont pour but de présenter les concepts et designs de façon claire et sont souvent soumis à des limites en terme de longueur. Cette section est donc dédiée à ajouter des précisions quant à la méthodologie suivie lors de la réalisation du projet ainsi que les détails relatifs à l'appareillage et les logiciels utilisés lors de la maîtrise.

L'idée de base du projet est d'étendre un concept de commande jusque là utilisé sur des robots de type portique qui sont découplés et ont une orientation constante à un robot sériel général à *n* degrés de liberté. Des simulations cinématiques fûrent donc effectuées à l'aide du logiciel *Matlab* afin de trouver un moyen de bien transformer une détection de mouvement autour d'une membrure à des mouvements correspondants des moteurs. Cette partie de la recherche initiale fait l'objet du premier article présenté dans ce mémoire au Chapitre 1.

Un prototype de robot sériel et de capteur à 3 degrés de liberté avaient déjà été conçus par les ingénieurs de recherche du laboratoire. L'algorithme de contrôle développé précédemment fut donc testé sur ce prototype afin de vérifier la fonctionnalité du concept ainsi que la stabilité de l'algorithme près des singularités. Le robot sériel utilisé est un prototype conçu et fabriqué pour ce projet. Il utilise des moteurs *Harmonic Drive* et des contrôleurs moteurs de marque *Elmo*. L'algorithme de contrôle est programmé à l'aide du logiciel *Simulink Real Time* qui communique avec le robot à l'aide du protocole de communication *EtherCAT*.

Ensuite un capteur de mouvement à 6 degrés de liberté a été conçu. L'architecture de base du capteur est inspirée de celle de la plate-forme de Gough-Stewart et des vérins spécialement conçus au laboratoire sont utilisés comme joints passifs élastiques. Des capteurs infrarouges sont utilisés afin de mesurer les déplacements des vérins. La conception de ce capteur de mouvement fait l'objet du deuxième article présenté dans le mémoire au Chapitre 2.

Ce capteur fut tout d'abord testé avec le robot à 3 degrés de liberté. Ensuite, deux autres moteurs furent ajoutés au robot afin d'obtenir un robot sériel à 5 degrés de liberté. Une fois celui-ci fonctionnel, le capteur put donc être testé pour des mouvements plus complexes dans un espace de travail plus représentatif de l'utilisation d'un tel robot.

Des tests ont finalement été effectués afin de comparer les performances de la méthode de contrôle à celle utilisée dans le robot commercial Kuka LRW. La comparaison est faite à l'aide d'un capteur de force et couple à 6 axes. Les résultats des différents tests effectués sont présentés dans les deux articles, par contre le Chapitre 1 se concentre sur la comparaison de la méthode avec celle utilisée pour le robot Kuka.

Le corps du mémoire présente donc diverses étapes de la méthodologie qui se complètent afin d'obtenir le résultat final qui est le robot collaboratif à 5 degrés de liberté.

Chapitre 1

A parallel low-impedance sensing approach for highly responsive physical human-robot interaction

1.1 Résumé

Cet article présente une nouvelle approche pour l'interaction physique entre un utilisateur humain et un bras robotique sériel. L'approche est inspirée du concept d'architecture macro-mini. La méthode est étendue pour un robot sériel à plusieurs degrés de liberté général et un schéma de contrôle correspondant est aussi proposé. Afin d'illustrer le concept, un bras robotique sériel à 5 degrés de liberté ainsi qu'un mécanisme de détection de mouvement à 6 degrés de liberté à faible impédance furent construits. Des résultats expérimentaux sont présentés.

1.2 Abstract

This paper presents a novel sensing approach for the physical interaction between a human user and a serial robotic arm. The approach is inspired from the concept of macro-mini robot architecture. The framework is developed for a general multi-degree-of-freedom serial robot and a corresponding impedance control scheme is proposed. In order to illustrate the concept, a five-degree-of-freedom robotic arm was built as well as a six-degree-of-freedom low-impedance sensing device that is used to control the robot. Experimental results are provided.

1.3 Introduction

Robots commonly used on assembly lines are usually not safe enough for humans to work near them or collaborate with them. In recent years, several research initiatives [27][16][5][11] have addressed

the development of safe robots that can physically assist humans on assembly lines as well as in daily life. Such robots must be safe, easy, and intuitive to use.

Many techniques can be used to make robots safer and easier to use [27]. Collision avoidance is perhaps one of the simplest where the robot changes path or stops completely if an obstacle is detected [3]. While this is very safe, it does not allow humans to really interact intuitively with the robot. Another way to make robots safer is to limit the robot speed and force. While this can also help making the robot safer, it does not make it easier to use or collaborate with and directly reduces the performance of the robot. Impedance control is a popular technique to enable the collaboration between humans and robots [23]. The user applies a force on the robot and moves it : this movement can be measured and used in a control law to make the robot follow a given behaviour. The drawback of this approach is that the user feels the impedance of the robot, which therefore needs to be low. Also, the user is directly in contact with the robot and mechanical limitations may be necessary.

One of the most popular approaches to safely enable human-robot collaboration is admittance control, which consists in using force/torque sensors to detect collisions or to gather feedback on the physical interaction between the robot and a human user [20][10][28]. In fact, this type of control can be thought of as a form of impedance control —with very high impedance— because the force measured is inferred from a displacement on a much smaller scale (usually the deformation of a strain gauge). In this case, the displacement required is so small that the robot virtually does not move. A drawback of this approach is that the user feels the delay of the control loop and that force or torque sensors are noisy and often suffer from drift.

Finally, another approach that is used to enable human-robot collaboration is the use of a macro-mini architecture [24][14]. In some implementations, the macro manipulator is an active manipulator while the mini manipulator is passive and is used to control the robot. In some cases, the mini manipulator also supports the payload [17][18][2]. The user moves the passive mini-manipulator which is a low-impedance mechanism, and the displacement between the macro and mini manipulators is used to control the actuated macro manipulator.

The drawback of the kind of macro-mini manipulators presented in [17][2] is that the low-impedance passive mechanism must support the weight of the payload and must be structurally robust. Furthermore, when interacting with the low-impedance mechanism, the user feels the inertia of the payload which has the effect of increasing the impedance of the mechanism if the payload is large.

A similar concept is presented here, where a low-impedance sensing device is mounted on the links of a serial robot. The user then physically interacts with the robot through a very low impedance mechanical port. Compared to existing collaborative robots in which the torques at the joints are measured (including the gravitational and inertial loads at the robot joints), the proposed approach has the advantage of directly measuring the interaction between the robot and user without ‘drowning’ the measurements in large gravitational loads. Moreover, instead of measuring the micro displacement of strain gauges (high impedance interface), the proposed approach relies on the measurement of

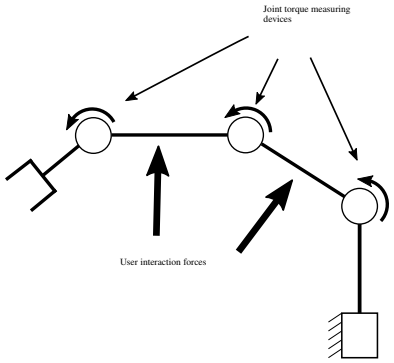

FIGURE 1.1 – Conventional collaborative robot with torque sensors at the joints.

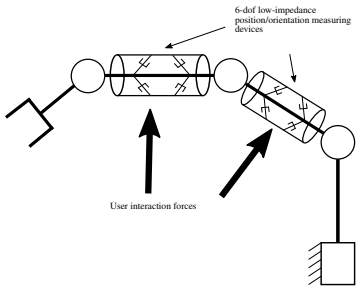

FIGURE 1.2 – Proposed collaborative robot with position/orientation sensors in parallel with the links.

displacements of the order of 1 cm, which yields a very low impedance and provides a very intuitive and immediate reaction. Also, compared to the macro-mini architecture, the proposed approach has the advantage of being independent from the payload and relying on small low-impedance components that do not play a structural role in the robot. The readings of the low-impedance sensing device are therefore limited to the user input and do not require any compensation or filtering. The new concept is detailed in this paper. Also, a six-degree-of-freedom (6-dof) sensing device and a 5-dof serial robot are developed and built in order to illustrate the application of the concept. Experimental results are also provided to demonstrate the effectiveness of the low-impedance interaction.

1.4 Conceptual Design

In conventional collaborative robots, the force applied by the user is inferred by measuring the joint torques, as illustrated in Fig. 1.1. In such an approach, the user interacts directly with a relatively high impedance system, which limits the reactiveness. As mentioned above, gravity and inertial loads due to the robot links and payload are included in the torque measured at the joints. These loads can be significantly larger than the loads produced by the user interaction, if a comfortable interaction is desired.

The idea behind the proposed concept, illustrated in Fig. 1.2, is to decouple the user interaction loads

from the gravitational and inertial loads of the robot and payload via low-impedance shells mounted on the links of the robot. The shells are connected to the robot via passive parallel mechanisms that are used to measure the displacement (position and orientation) of the shells with respect to the links. The passive parallel mechanisms are equipped with elastic return devices that return to the reference configurations when no external load is applied to the shells. Using this arrangement, the user loads are decoupled from the gravitational and inertial loads due to the robot and the payload. By using the low-impedance sensing devices to measure the position and orientation of the shells with respect to the robot links, the interaction with the user has a low impedance which allows for a high responsiveness. The motion of the shells is mapped into the motion of the robot using a procedure that is explained in the following sections.

1.5 Passive Displacement Measurement

Robotic manipulators typically have a high impedance, especially compared with humans. Therefore, the physical interaction of a human user with a robot can feel rather unnatural. By using a passive low-impedance mechanism mounted on a high impedance mechanism (the structure of the robot), the bandwidth can be greatly enhanced. In order to understand the advantages and limitations of this concept, a one-degree-of-freedom kinematic model is first developed.

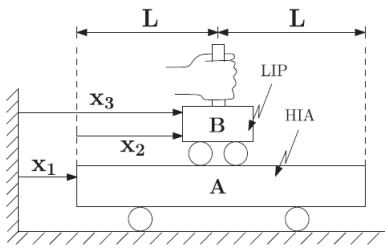

FIGURE 1.3 – Representation of the one-degree-of-freedom macro-mini manipulator, figure taken from [17]

.

1.5.1 Kinematics of a one-degree-of-freedom active-passive system

Consider the macro-mini active-passive system shown in Fig. 1.3. A low-impedance passive (LIP) mechanism B moves with respect to a high-impedance active (HIA) mechanism A on which it is mounted. The equations of this 1-DOF mechanism have been introduced in [17] and are briefly recalled here. The position of the passive mechanism with respect to the ground is given by

$$x_3 = x_1 + x_2 \tag{1.1}$$

where x_1 is the position of the active manipulator and x_2 is the position of the passive mechanism relative to the active manipulator.

In order to obtain the frequency response of the system, a harmonic motion is applied to the passive manipulator by the human user, namely

$$x_3 = R\sin(\omega t) \tag{1.2}$$

where R is the amplitude of the movement, ω the frequency, and t the time. The system is designed to keep the relative position x_2 at a mid-range value. To accomplish this, the macro manipulator must move with a frequency identical to that of the input and the movement can be described as

$$x_1 = D\sin(\omega t) \tag{1.3}$$

where D is the amplitude of the movement. If the passive mechanism starts from a midpoint, where L is the maximum range of motion that it can perform relative to the active manipulator and the passive mechanism has a movement amplitude R greater than L, the active manipulator must move accordingly with an amplitude of

$$D = R - L. \tag{1.4}$$

Given the limitations on the velocity and acceleration of the active system, noted $\dot{x}_{\max,1}$ and $\ddot{x}_{\max,1}$, the maximum amplitude of motion of the active system can be found, namely

$$D^v_{\max} = \frac{\dot{x}_{\max,1}}{\omega} \quad , \quad D^a_{\max} = \frac{\ddot{x}_{\max,1}}{\omega^2} \tag{1.5}$$

and hence the maximum input amplitude that can be accommodated without exceeding the physical limits of the passive mechanism, noted $R_{\max}$ can then be found from (1.4)

$$R^v_{\max} = \frac{\dot{x}_{\max,1}}{\omega} + L \quad , \quad R^a_{\max} = \frac{\ddot{x}_{\max,1}}{\omega^2} + L. \tag{1.6}$$

For a given amplitude of input motion R, (1.6) can be used to characterize the bandwidth of the system, which depends on the maximum velocity and acceleration of the active component and on the range of motion of the passive mechanism, L. If the system is responsive enough, the user never reaches the motion limits of the passive mechanism and the interaction always remains very intuitive [2]. This is a direct benefit of using a low-impedance passive interface with a relatively large range of motion [1] between the user and the robot. The passive range of motion, noted L in (1.6), contributes greatly to increasing the bandwidth of the interaction.

1. A range of motion in the order of 1 cm is used here.

1.5.2 Application to a general serial robot

The expressions found in the previous section are obviously not directly applicable to a multi-DOF serial robot unless the robot is completely decoupled. In most serial manipulators, the values of $\dot{x}_{\max}$ and $\ddot{x}_{\max}$ are dependent on the configuration of the robot. The relation between the Cartesian velocity vector $\mathbf{t}$ and the actuator velocity vector $\dot{\boldsymbol{\theta}}$ is given by

$$\boldsymbol{t} = \boldsymbol{J}\dot{\boldsymbol{\theta}} \tag{1.7}$$

where $\boldsymbol{J}$ is the Jacobian matrix and where the joint velocity vector is constrained as

$$\dot{\boldsymbol{\theta}} \preceq \dot{\boldsymbol{\theta}}_{\max} \tag{1.8}$$

where $\preceq$ stands for the componentwise inequality. For a given configuration of the robot, (1.7) and (1.8) define a polytope that provides the Cartesian velocity limits [19]. This polytope can be used to determine the capabilities of the robot in a given Cartesian direction, which can then be used in 1.6 to determine the bandwidth provided by the low-impedance sensor. This can be used when planning a task to see what configuration would be the most suitable for the robot, similarly to how one would use the sensitivity index to plan a precise task. A similar analysis can be done for the accelerations of the robot.

1.6 Control scheme

1.6.1 Control loop

The basic inner control loop is based on a simple position controller. The position error can be expressed as

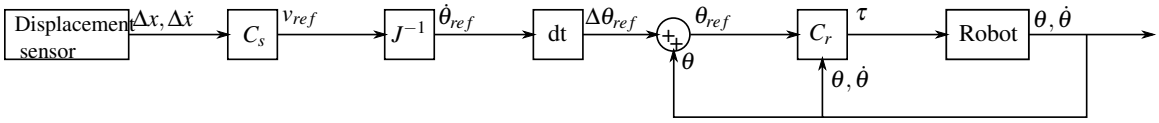

FIGURE 1.4 – Control loop of the system. C_s is the controller used on the sensor displacement and C_r is the low-level position controller.

$$\boldsymbol{e} = \boldsymbol{\theta}_{ref} - \boldsymbol{\theta} \tag{1.9}$$

where $\boldsymbol{\theta}_{ref}$ is the desired position vector and $\boldsymbol{\theta}$ is the actual joint coordinate vector. This error is used in a controller to obtain a torque to control the motors, namely

$$\boldsymbol{\tau} = \boldsymbol{K}_p\boldsymbol{e} + \boldsymbol{K}_d\dot{\boldsymbol{e}} + \boldsymbol{g}(\boldsymbol{\theta}) \tag{1.10}$$

where $\dot{\boldsymbol{e}}$ is the time derivative of the position error and $\boldsymbol{g}(\boldsymbol{\theta})$ is the gravity compensation term. $\boldsymbol{K}_p$ and $\boldsymbol{K}_d$ are the proportional and derivative coefficient matrices respectively. If the robot is used to follow a prescribed trajectory, then $\boldsymbol{\theta}_{ref}$ is prescribed by a trajectory planning algorithm. However, if the robot is controlled using the passive interaction mechanism, determining the appropriate value of $\boldsymbol{\theta}_{ref}$ requires some pre-processing. In this case, the displacement of the passive mechanism can be used to obtain a reference velocity as

$$\boldsymbol{v}_{ref} = \boldsymbol{K}_{ps}\Delta\boldsymbol{x} + \boldsymbol{K}_{ds}\Delta\dot{\boldsymbol{x}} \tag{1.11}$$

where $\boldsymbol{K}_{ps}$ and $\boldsymbol{K}_{ds}$ are respectively the proportional and derivative coefficient matrices and $\Delta\boldsymbol{x}$ and $\Delta\dot{\boldsymbol{x}}$ are the displacement of the low-impedance sensing device and its time derivative.

The Cartesian reference velocity obtained from (1.11), $\boldsymbol{v}_{ref}$, is then mapped onto the joint space of the robot using the Jacobian matrix $\mathbf{J}$ of the robot, namely

$$\dot{\boldsymbol{\theta}}_{ref} = \boldsymbol{J}^{-1}\boldsymbol{v}_{ref}. \tag{1.12}$$

The prescribed position in the joint space $\boldsymbol{\theta}_{ref}$ is then obtained by integrating the velocity over one time step and the resulting value of $\boldsymbol{\theta}_{ref}$ is used in the motor controllers to move the robot. In summary, the measured displacement of the shell mounted on a link is used to calculate a velocity command which is then integrated and used as a control input for the low-level position control of each of the motors. The global control scheme is illustrated in Fig. 1.4.

1.6.2 Mapping of the desired motion onto the joint space and use of the damped pseudo-inverse

The above derivation assumes that the robot is not in a singular configuration. It also assumes that the number of degrees of freedom of a given link, on which the low-impedance shell is mounted, matches that of the connection (displacement sensor) mounted between the shell and the link. However, in the proposed implementation, 6-dof passive mechanisms are used to connect the shells to the links, even for links that have fewer than 6 degrees of freedom. Therefore, in such cases, the Jacobian matrix associated with the link on which the sensor is mounted has fewer columns than rows. For instance, consider the third moving link of a serial robot. The Jacobian matrix associated with this link has 6 rows and 3 columns. If a 6-dof displacement sensor is mounted on this link, the displacements measured by the sensor are generally not compatible with the available three dofs and have to be mapped onto the motion that can be produced by the first three joints of the robot to produce the required motion as closely as possible. Equation (1.12) is then replaced with

$$\dot{\boldsymbol{\theta}} = (\boldsymbol{J}^T\boldsymbol{J})^{-1}\boldsymbol{J}^T\boldsymbol{t} \tag{1.13}$$

which is the least square solution to (1.7). The resulting joint motion produces the Cartesian motion that is as close as possible to the requested motion, in the sense of the least squares, which produces an intuitive behaviour.

Additionally, in singular configurations, matrix $\boldsymbol{J}$ becomes rank deficient. In this case, even the formulation of (1.13) fails. In order to alleviate this problem, the concept of damped pseudo-inverse [8] is used.

Indeed, near singular configurations the joint velocities required in order to produce a certain Cartesian velocity can become very high which is not desired, especially when dealing with collaborative robots. The solution based on the damped pseudo-inverse can be expressed as

$$\dot{\boldsymbol{\theta}} = (\boldsymbol{J}^T\boldsymbol{J} + \alpha\boldsymbol{I})^{-1}\boldsymbol{J}^T\boldsymbol{t} \tag{1.14}$$

where α is the damping coefficient and $\boldsymbol{I}$ is the identity matrix. The formulation of (1.14) is very similar to that of (1.13). In fact, it is identical if α is equal to zero, but the addition of the damping term $\alpha\boldsymbol{I}$ prevents the matrix from becoming singular which stabilises the solution. Parameter α is generally tuned experimentally on the real robot and it can also be modified online by using the condition number of the Jacobian matrix.

1.7 6-dof displacement sensor

One of the challenges of this project is to design a sensor able to detect the movements of the shells in all 6 degrees of freedom. The sensors must be mounted around the structural links of the robot and provide a proper range of motion in all directions while avoiding mechanical interferences. The user must be able to manipulate the sensor as if it were part of the links of the robot in order for the interaction to feel natural. Also, the sensing mechanism must automatically return to its neutral reference configuration when no external load is applied on it.

1.7.1 Architecture

The sensor must be a passive mechanism able to detect movement in all 6 axes. Parallel mechanisms are well suited for this kind of application [2]. The passive mechanism must have a stable neutral configuration, which can easily be achieved with a parallel mechanism. The parallel mechanism also has the advantage of requiring smaller position sensors since they are all independently connected to the end effector and need not to support the weight of other sensors.

The architecture chosen for the sensor is based on the Gough-Stewart platform [26]. This architecture has several features that are advantageous for our application. First of all, it is possible to arrange the attachment points of the base (robot link) and the effector (shell) in two concentric circles. The other feature is the great stability of the platform around its neutral position. Since the robot is always trying to follow the motion measured by the sensors —i.e., trying to keep the sensing mechanism in its

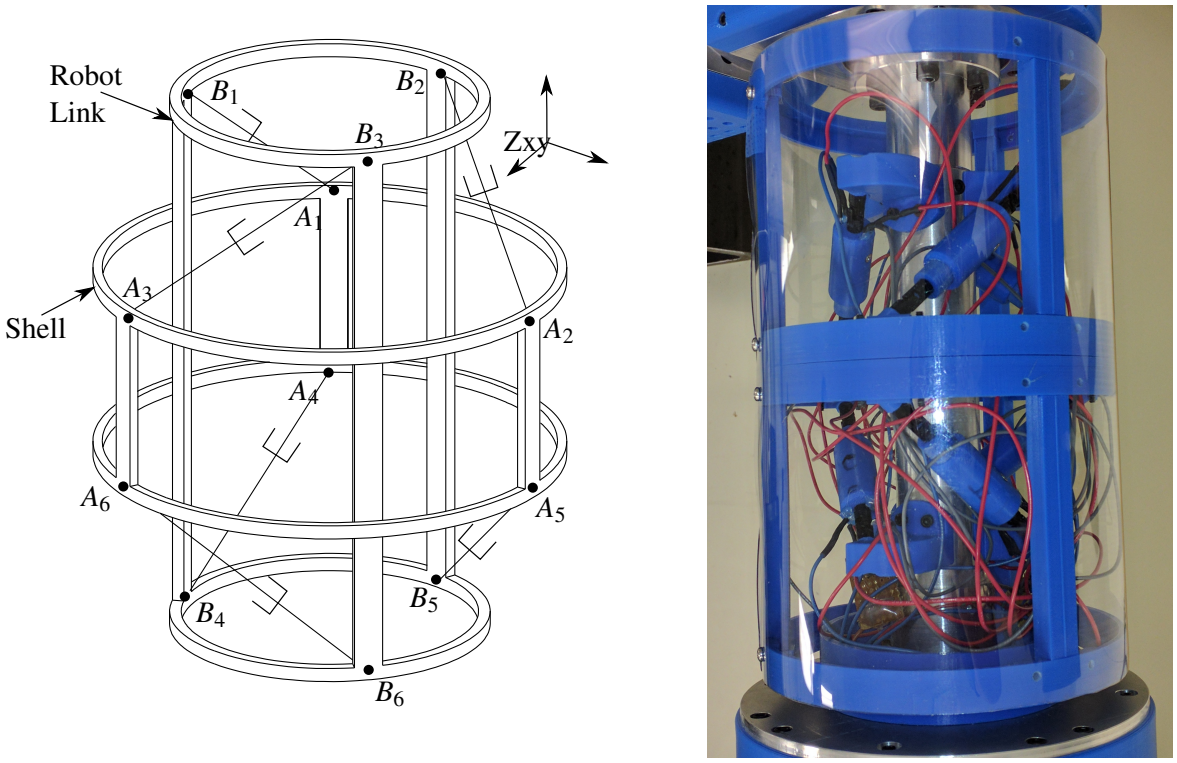

FIGURE 1.5 – Architecture of the displacement sensor, where B_i is the ith attachment point on the robot link and A_i is the ith attachment point on the mobile shell. The line connecting A_i and B_i represents the spring-loaded linear position sensors. A photograph of the prototype is shown on the right hand side.

neutral configuration—, the range of motion of the passive mechanism does not need to be too large with respect to the size of the mechanism. Therefore, a stable mechanism is an advantage. Finally, even with relatively small linear sensors and corresponding mechanical limits, the mechanism can take relatively large loads due to the parallel architecture. Springs are used in the linear sensors to return the mechanism to its neutral configuration when no external load is applied. The stiffness of the springs and the preload is adjusted to ensure that the mechanism does not move under the effect of the weight of the shell and that the interaction forces perceived by the user are appropriate.

The architecture of the Gough-Stewart platform is modified in order to have the effector around the base instead of over it. Indeed, in a standard Gough-Stewart architecture, all the attachment points on the effector are located on a plane and all of the attachment points of the base are located on another plane. Here, the architecture is modified such that the points of attachment on the platform (here the shell) are distributed on two planes and the attachment points on the base (link) are located on both sides of the points on the platform. This allows for a better use of the space and makes the mechanical design easier. The final architecture is shown in Fig. 1.5 together with a photograph of the prototype.

1.7.2 Geometric design

The starting point of the geometric design of the sensor is the design of the passive linear sensors that connect points A_i and B_i. The linear position sensors are preloaded cylinders having a range of motion of ± 8 mm and a rest length of 63 mm. The motion range chosen for the sensor is 1 cm in each direction, therefore the attachment points must be chosen to maximise the use of the cylinders' range of motion.

In order to find a proper set of attachment points, the inverse kinematics of the parallel platform is used. The geometric constraints of the platform can be expressed as

$$\rho_i^2 = (\boldsymbol{a}_i - \boldsymbol{b}_i)^T (\boldsymbol{a}_i - \boldsymbol{b}_i) \tag{1.15}$$

where ρ_i is the length of cylinder i, $\boldsymbol{a}_i$ is the position vector of the shell attachment point of cylinder i, and $\boldsymbol{b}_i$ is the position vector of the base attachment point of the cylinder i. The vector positions $\boldsymbol{b}_i$ are constant when expressed in the base (link) frame while the positions $\boldsymbol{a}_i$ can be expressed as

$$\boldsymbol{a}_i = \boldsymbol{p} + \boldsymbol{Q}\boldsymbol{a}_{t,i} \tag{1.16}$$

where $\boldsymbol{p}$ is the position of the reference point of the shell, $\boldsymbol{Q}$ is the rotation matrix applied to the shell, and $\boldsymbol{a}_{t,i}$ is the position vector of the shell attachment point of cylinder i in the shell frame of reference. For a given geometric architecture, i.e., for given base attachment points and shell attachment points, it is easy to apply displacements and rotations and verify whether the length of the cylinders corresponds to their physical limits. It is then possible to adjust the position of the base points or shell points to maximise the use of the cylinder.

One architecture that was found that satisfies the above constraints is shown in Fig. 1.5.

The last step is to ensure that the actual mechanical assembly does not interfere with any of the other robot parts. This is easily accomplished using movement simulations in a CAD software or custom programs with simple geometric shapes.

1.7.3 Determination of the Cartesian displacement of the sensor

In the proposed concept, the user applies a force on the sensor, which makes it move. Infrared distance sensors in the cylinders are used to measure the length of the cylinders and these lengths can be used to compute the direct kinematics of the Gough-Stewart platform constituting the sensor and find the displacement of the shell.

The solution of the direct kinematics of a parallel mechanism has been studied in many references [22][25][21]. Numerical solutions are available, for example using the Newton-Gauss algorithm [1]. Moreover, in this application, the mechanism is always relatively close to the reference configuration

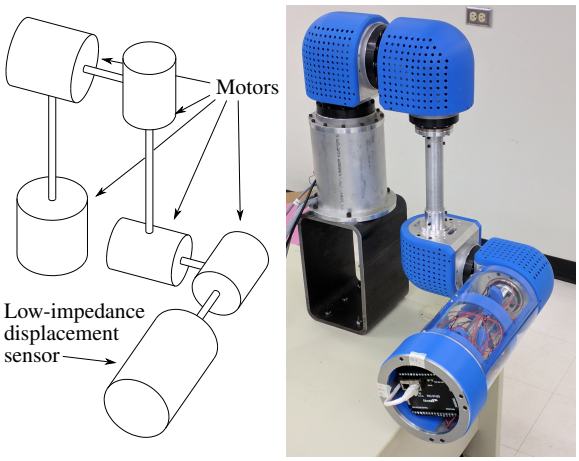

FIGURE 1.6 – Architecture of the experimental 5-dof robot with the low-impedance displacement sensor.

and does not reach singular configurations, which ensures that the numerical procedure always converges and is very efficient.

1.8 Experimentation

In order to demonstrate the proposed concept, a prototype of the sensor presented above was built along with a 5-dof serial robot.

1.8.1 Robot architecture

As previously stated, the sensor was tested on a 5-dof robot despite having 6 dofs. Using a robot that has fewer dofs than the sensor itself brings a few interesting challenges but also allows to demonstrate the effectiveness of the mapping algorithm presented in section 1.6.2. The general architecture of the robot is presented in Fig. 1.6. The architecture is based on two clusters of motors : one with three motors and the other with two motors. It is planned to extend the robot to a 7-dof architecture in the future.

1.8.2 Experimental validation

As shown in Fig. 1.6, the prototype of the sensor was mounted on the last link of the 5-dof robot and tests were conducted to assess the performance of the proposed concept. The first basic way to measure the performance of the robot is to simply measure the difference in position in the Cartesian space between the sensor and the robot. This allows us to measure the reactiveness of the system and to ensure that the robot can follow the input from the sensor without the sensor reaching its mechanical limits.

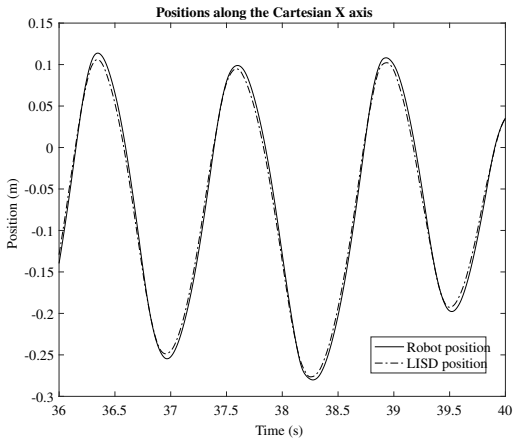

FIGURE 1.7 – Position of the link and Low Impedance Sensing Device (LISD) along the x axis for an oscillating motion.

As seen in Fig. 1.7, the robot is able to follow the motion of the sensor well, so that the sensor never reaches its mechanical limits. The largest position difference is approximately 8 mm whereas the maximum movement allowed for the sensing device is 10 mm. The largest differences occur when the acceleration is at its highest because while the user can move the sensing device quickly due to its low impedance, the robot's reaction will be slightly slower due to its high inertia. However, since the sensor does not reach its mechanical limits, the lagging of the robot is not felt by the user and the interaction continues to be very intuitive and smooth during the high acceleration phases of a trajectory.

One of the main features of the approach used in this paper is, as stated previously, the very low impedance of the sensing device. This allows the user to move the robot using a very small force. The force required to move the robot is compared to the force required to move a Kuka LWR robot. A force sensor is mounted on each robot and used to input a force on the robot which in turn generates a movement.

The results of the experiments conducted with the two robots are shown in Fig. 1.8, where the interaction force and the velocity of the robot are plotted as a function of time for an oscillating motion. It can readily be observed from the figure that approximately twice as much force is necessary in order to produce similar speeds at a similar frequency with the Kuka LWR robot. Since the displacement sensor has a very low impedance, the force required to produce a given acceleration is lower and this force can be tuned by changing the pre-load or the springs used in the passive mechanism. Another important observation is the phase difference between the velocity and the force applied. For the Kuka LWR, the velocity lags behind the force applied due to its higher impedance, whereas the sensing device's velocity almost stays in phase with the force. The phase difference for the Kuka LWR in Fig. 1.8 is between 0.11-0.18s and for the LISD it is between 0.07-0.1s. Having a small phase difference between the applied force and the movement is directly related to the comfort of the user. When

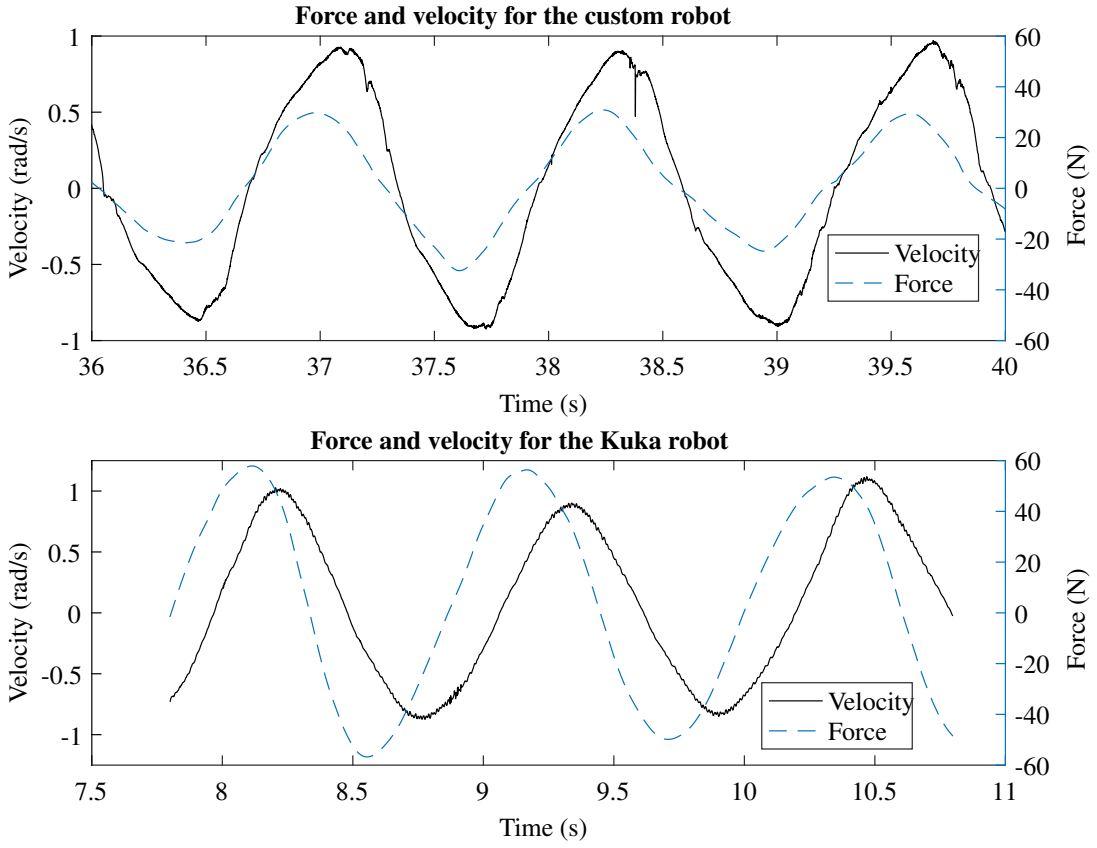

FIGURE 1.8 – Force and velocity graph comparison between the sensing device and the Kuka LWR for a similar movement using only the first 5 joints of the Kuka LWR robot.

the phase difference is large, the user may feel as if he is fighting the robot when trying to apply an acceleration. A smaller phase difference means a much more responsive feeling and a better sense of control on the movement. When working for a longer period of time with the robot, the large phase difference can become tiring for the user because he will feel like he is trying to move a large inertia. These results illustrate the benefit of a low-impedance interface, which is confirmed by the comfort perceived during the experimental tests.

1.9 Multimedia Extension

A video accompanying this article demonstrates the experiments performed with the robot and sensor. The video demonstrates the ability to move the robot within its workspace without much effort using the sensing device. It also demonstrates slow and precise movements, high-speed movements and accelerations, as well as stability when performing oscillating movements or step movements.

1.10 Conclusion

A concept of low-impedance position sensor for the intuitive physical human-robot interaction was presented in this article. The concept was first described and the advantages of a low impedance interface for the intuitivity of the interaction were highlighted. The controller used to implement the concept was then briefly presented. The low-impedance position sensor, which is based on a Gough-Stewart platform architecture was then introduced. Finally experiments conducted with a 5-dof robot on which the 6-dof sensor was mounted were reported. The effectiveness of the concept was demonstrated by comparing the interaction forces with those measured while interacting with a Kuka LWR robot and noting the improved tracking characteristics. Future work includes the extension of the robot to a 7-dof architecture and the integration of low-impedance sensors on all of its links.

Chapitre 2

Mechanical design and experimental validation of a low-impedance 6-degree-of-freedom displacement sensor for intuitive physical human-robot interaction

2.1 Résumé

Cet article présente le design mécanique d'un capteur de déplacement à faible impédance (LIDS) à six degrés de liberté capable de mesurer trois translations et trois rotations. Le capteur est installé autour d'une membrure de robot sériel et utilisé comme interface pour une interaction humain-robot. Le design mécanique des composantes élastiques est d'abord présenté. Ensuite, l'architecture ainsi que la cinématique du capteur sont introduites et la cinématique directe et inverse sont résolues. Une analyse de la sensibilité cinématique est ensuite réalisée afin de caractériser la précision du mécanisme. Finalement, le design du prototype final est présenté ainsi que les résultats expérimentaux.

2.2 Abstract

Résumé

This paper presents the mechanical design of a six-degree-of-freedom Low-Impedance Displacement Sensor (LIDS) able to measure displacement along three axes in translation and rotation. The sensor is mounted around a link of a serial robot and used as an interface for physical human-robot interaction. The motivation for the use of a low-impedance sensor is first discussed. The mechanical design of the elastic components of the sensor is then presented. The kinematic architecture of

the mechanism is introduced and the inverse and forward kinematic problems are solved. The kinematic sensitivity is then used to characterize the accuracy of the mechanism. Finally, the design of a prototype is presented and experimental results are provided.

2.3 Introduction

As collaborative robots become more common in industry, the need for intuitive and safe control methods also increases. When dealing with automation on assembly lines for instance, it can be easy to separate the robots from the human operators to ensure safety. For some tasks however, a combination of humans and robots can produce better performance. In order to accomplish such tasks, the user needs an intuitive and safe method to command the robot. Various methods can be used to ensure the safety of collaborative robots [27, 16, 5, 11].

Recently, different techniques have been proposed in order to let a human user directly manipulate a robot. These control approaches, known as impedance [23] and admittance [20] control, allow a user to apply a force directly on the robot, which then uses encoders or force sensors to infer the intentions of the user and responds with appropriate motion. These methods are intuitive and already in use in various commercial robots such as the Kuka LBR IIWA [1] or the Universal Robot UR-5 [2]. While being intuitive and relatively safe, these methods often have a rather narrow bandwidth and using them for extended periods of time can be strenuous. Furthermore, the user still interacts directly with the structure of the robot and some force and velocity limitations are needed.

Another approach, which is closely related to the one presented in this paper, is to use a macro-mini architecture [18, 2]. This method uses an additional passive mechanism mounted between the payload and the active manipulator. The user interacts with the payload instead of the robot and the passive mechanism, which has a low impedance, monitors the movements of the payload using position sensors and sends commands to the active manipulator. This method offers a very intuitive control to the user and since there is no need to interact directly with the active (macro) manipulator, it is safer than conventional impedance or admittance control. One drawback of this approach is that the passive mechanism must support the payload. This means that the mechanism must be sturdy — and hence possibly bulky — and that counterweights may have to be used to support larger payloads. It is also worth noting that for heavier payloads, even if the mechanism itself has a low impedance, the user still feels the inertia of the payload.

The mechanism presented in this paper is inspired from the macro-mini architecture. However, instead of mounting the passive mechanism between the payload and the active mechanism, it is mounted on the robot's links, between the link and an outer lightweight shell. The user can then interact with the lightweight shell — instead of interacting directly with the structure of the robot — and the relative motion between the shell and the link is measured by the passive mechanism. This drastically reduces

1. https ://www.kuka.com/en-ca/products/robotics-systems/industrial-robots/lbr-iiwa
2. https ://www.universal-robots.com/products/ur5-robot/

the mechanical impedance of the interaction between the user and the robot, thereby greatly increasing the bandwidth. This approach can be used on a serial robotic arm since the proposed mechanism can be mounted around any link of a robot.

This paper is structured as follows. The principle of the proposed approach is exposed in Section 2 and the mechanical design of the elastic prismatic joint sensors is presented in Section 3. The kinematic and static analyses of the mechanism are given in Section 4 while Section 5 describes the prototype and the experimental validation. Finally, Section 6 presents some experimental results.

2.4 General Approach and Motivation

The goal of the mechanism developed in this paper is to be able to measure movements along different axes in both translation and rotation with up to 6 degrees of freedom in order to capture the motion imparted to the outer shell of a robot link by a human user. In this framework, the mini mechanism is the passive mechanism and the macro mechanism is the robot itself. The macro-mini approach was successfully used in the literature with gantry manipulators due to their ease of control and decoupled nature. With often only 3 translations, some decoupled mechanisms such as the Tripteron [2] can be used to sense the motion of the effector and control the gantry system. However, it is required here to control a multi-degree-of-freedom serial robot which can include rotations as well as translations. This poses another challenge since the mini mechanism itself changes orientation during the operation, which prevents the use of counterweights that operate based on gravity (as demonstrated in [18, 2]) to produce the return action of the mini mechanism. Indeed, a return action is required on the mini mechanism so that the robot stops moving when the user lets go of the outer shell of the links. Furthermore, the mini mechanism must be mounted around a robot link and be accessible and easy to use. This can be accomplished using various techniques and tools. The choice of architecture and sensing methods are fundamental components of the design of the mechanism and are explained in the following sections.

2.4.1 Passive Elastic Parallel Mechanism

Mechanisms can not only be used as manipulators but also as displacement sensors. By knowing the kinematics of a given mechanism and the joint coordinates, it is possible to determine the position of the end effector using the forward kinematic transformation. For serial manipulators, this is particularly easy because the forward kinematics are usually straightforward and yield only one solution. Serial mechanisms, however, have a few major drawbacks making them less suitable for position sensing in some cases. The goal of the sensor being to control a robot using a low-impedance interface, the sensor itself needs a stable mid-range configuration to which it returns when no force is applied. This can be implemented in a serial mechanism, but it can be difficult especially when dealing with multiple degrees of freedom. The other drawback of serial mechanisms is their limited ability to provide a light-weight architecture. Indeed, in a serial mechanism, the links that are closer to the base

must support the weight of the other links which adds more mass to the overall mechanism. This mass increases the inertia, yielding a higher impedance and the need for stronger passive elastic joints to return the mechanism to the mid-range configuration when no force is applied. Clearly, the simple forward kinematics of serial mechanisms are not enough to justify their use, given the mechanical drawbacks of such mechanisms.

Parallel mechanisms on the other hand, have very simple inverse kinematics but the forward kinematics can become very complex and numerical techniques are often employed to solve them. However, the mechanical advantages that they provide can justify their use. Within the wide variety of possible parallel mechanisms, it is easy to find some that are very stable around a mid-range configuration. The other major advantage is that each of the legs only needs to support a part of the weight of the effector and not the weight of the rest of the mechanism. This means that smaller elastic joints are required and the mechanism itself therefore has a smaller mass, which yields a smaller impedance and better feeling for the user. Parallel mechanisms also offer many possibilities for joint sensing depending on the type of joint used in the mechanism. A parallel architecture is therefore chosen for this sensor design. The architecture is based on the Gough-Stewart platform architecture [26], which is relatively simple to implement mechanically and offers some great advantages.

2.4.2 Single axis displacement measurement

As mentioned above, the Gough-Stewart platform is chosen for the architecture of the parallel mini mechanism used to measure the displacements and rotations around a mid-range configuration. In this mechanism, elastic return is ensured by spring-loaded prismatic joints and the length of the legs is measured in order to determine the displacement and rotation of the platform. Various techniques can be used to measure a displacement along one direction such as linear or rotational encoders, potentiometers, and various optical sensors. Load cells, which are used to indirectly measure forces, are in fact displacement sensors at a very small scale [3]. The single axis displacement measurement is used to determine the movement of the passive prismatic joints of the mechanism. These measurements are then used to calculate the position and orientation of the end-effector using a numerical technique described in Section 5, namely a numerical solution of the direct kinematic problem.

One of the most common means of measuring distances without contact is to use optical sensors. There exists a wide variety of optical sensors that can measure movements in the range of the μm (optical micrometres) up to hundreds of metres (laser rangefinders). In the present application, the movement induced by the user should be of the order of a few centimetres, which corresponds to a similar movement of the passive prismatic joints. One of the best options to measure distances within this range is to use an infrared photoresistor with an infrared LED. Some of these sensors have a few centimetres of range and can be adjusted using a reflective surface and the proper combination of resistors. They are inexpensive and easy to use and integrate mechanically. The one drawback of these sensors is the sensitivity to external light. Sunlight for instance, drastically affects the measurements

3. Displacements of the order of μm.

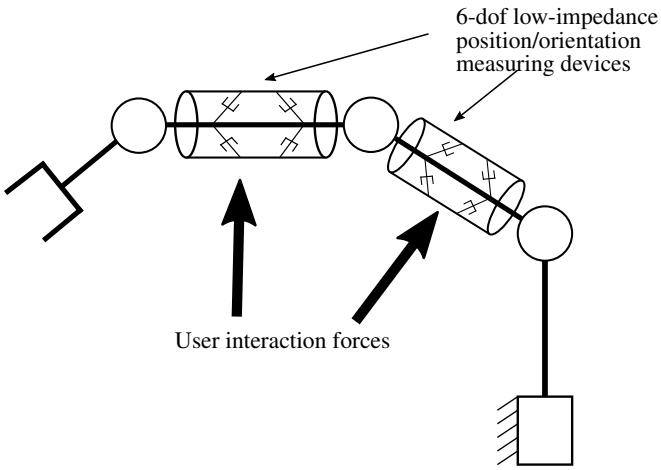

FIGURE 2.1 – Conceptual design of the mechanism mounted on a serial robot.

provided by photoresistors because it contains wavelengths covering a wide spectrum. It is therefore important to properly isolate the sensor from external light.

2.5 Architecture

The 6-dof sensor must be mounted on a robot link and it must cover most of its surface as shown schematically in Figure 2.1. In order to match this constraint, the general architecture of the sensor is composed of a mobile lightweight cylindrical shell connected to the robot link by 6 passive prismatic joints mounted on Hooke joints and spherical joints.

The architecture of the serial robot on which the sensor is to be mounted was determined before that of the sensor, which means that the dimensions of the robot must be satisfied in order to avoid mechanical interferences. Therefore, the shell's diameter must not be too large while leaving enough space for the passive prismatic joints to move. The other major consideration is the size of the robot link, which was determined from the payload capacity and the weight of all components (actuators, links). Therefore, because the sensor is mounted around the link, it must be small enough to leave space for the joints of the sensor to move.

An important design decision is to determine the magnitude of the allowed displacement of the shell. Very small displacements, such as those of force sensors, yield a very high impedance, which is not desired. On the other hand, very large displacements can make the robot feel sluggish and the sensor might end up being too heavy and bulky. A reasonable compromise was found with displacements of 1cm in all directions. Based on the kinematic analysis presented in [2] and on the acceleration capabilities of the robot, it can be shown that such displacements provide relatively high velocity and acceleration of the shell without reaching the mechanical limits of the prismatic joints.

Both the sensor architecture and the passive joints are designed based on these constraints, as discussed

in subsections 3.1 and 3.2.

2.5.1 Passive Prismatic Joints

The passive elastic prismatic joints included in the design of the sensor must support the outer shell — which is in fact the moving platform of the Gough-Stewart mechanism — and keep the mechanism in its neutral configuration for any orientation of the robot link. Furthermore, each prismatic joint must enable movements of approximately 1cm of the shell. One last constraint for the joint is that it must be able to house a photoresistor used to measure the displacement of the joint. The photoresistor must also be located inside the cylinder and shielded from outside light to prevent noise in the signal provided by the sensors.

The basic design for the passive prismatic elastic joint is a spring-loaded cylinder. Each leg of a Gough-Stewart platform must allow 6 degrees of freedom, including the prismatic joint, a universal joint at each end of the cylinder and allowing rotation along the main axis of the cylinder.

Since the prismatic joint must move around a mid-range (neutral) configuration, the spring must be able to return the joint to this neutral configuration independently from the direction of motion. Different approaches can be used to obtain such a behaviour. An obvious design would be to use two springs, one for each direction. This concept is shown in figure 2.2. One side is used for compression movements while the other is used for extension movements. Having two springs can be useful for some applications where the desired behaviour is different in compression or extension. One drawback however is that, in applications where the same behaviour is desired in both directions (like the one considered in this paper), it is hard to guarantee uniformity because both springs must have exactly the same properties (stiffness and preload). Figure 2.3 shows the concept used in this paper. This concept uses a single shaft and a single spring, as well as two mobile parts that move relatively to each other to compress the spring depending on the direction of the movement. This design guarantees the same behaviour in both directions of the movement. It is also easier to measure the displacement by simply measuring the position of the central shaft. Furthermore, this design is more compact since it uses only one spring. Indeed, the space required for the spring must be larger than range of motion of the joint. This is required because the compression spring has a maximum compression physically possible. In the single-spring configuration, this extra space is only needed once because the same spring is used for both directions.

The design of the passive spring-loaded prismatic joint is presented in Fig. 2.4. In order to use only one compression spring, the cylinder is built using a combination of 4 parts moving with respect to one another. The base Hooke joint (Universal joint) is fixed on the housing of the cylinder whereas the shell Hooke joint is fixed on the central shaft of the cylinder. The optical distance sensor and the reflective surface are also positioned respectively on the housing and the central shaft. When pushing on the cylinder, the shell's universal joint is pushing on the floating part 1 as well as the central shaft. The floating part 1 then compresses the spring on the 2nd floating part and the housing of the cylinder.

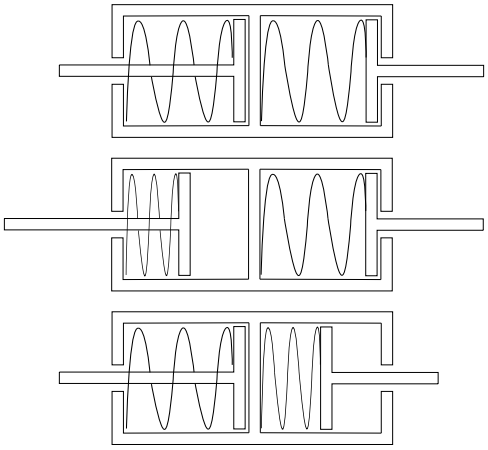

FIGURE 2.2 – Conceptual design of the cylinder with two compression springs shown at the neutral point, in extension, and in compression.

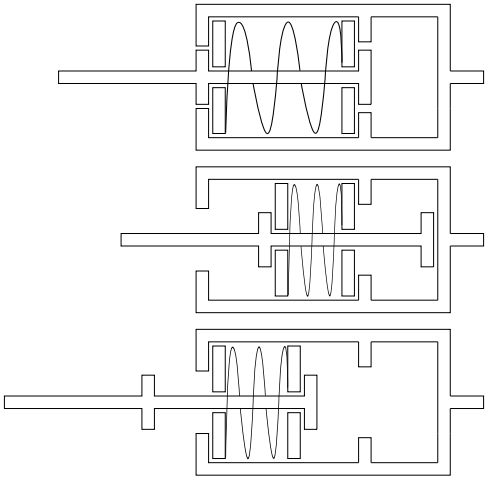

FIGURE 2.3 – Conceptual design of the cylinder with a single compression spring shown at the neutral point, in compression, and in extension.

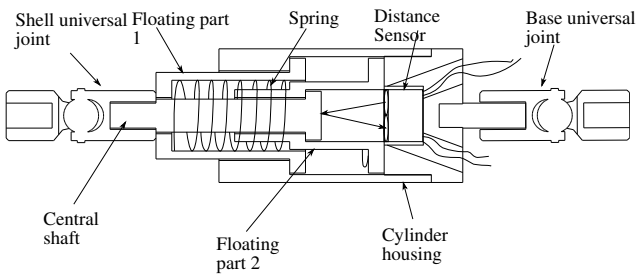

FIGURE 2.4 – Section view of the passive prismatic joint used for the sensing mechanism.

When pulling on the cylinder, the shell's universal joint pulls the central shaft which in turn pulls the 2nd floating part. This part then compresses the spring on the first floating part and the housing of the cylinder. This design uses the same space for both directions and uses only one spring, thus reducing the overall length of the cylinder itself.

The final dimensions of the joints such as the midpoint length and range were determined using the final architecture of the sensor which is described in the next section.

2.5.2 Mechanism Architecture

As previously stated, the architecture of the sensor is based of the Gough-Stewart platform [26]. This choice was made because it is a very effective architecture and it is very stable around its mid-range (neutral) configuration, which is a desirable behaviour. It also uses prismatic joints, which were previously designed with this use in mind.

The standard Gough-Stewart architecture usually has the end effector over the base with all the attachment points of the base located on one plane and those of the effector located on another plane. For the sensor, the effector —which is the mobile shell— is located around the base, which is the robot link. The standard Gough-Stewart architecture could work as a movement sensor. Indeed, one could place the base points around the link on a small circle and the shell points on a larger circle on a different plane. However, this would not be the most efficient use of the space available around the robot link. In order to provide the best behaviour, the shell's centre of rotation must be in the centre of the link. By using the standard Gough-Stewart architecture, all the legs end up on the same side of the centre of the link and only half the space is used. Although this could work from a kinematic point of view, mechanical interferences and other packaging issues arise. Furthermore, to facilitate the integration of the sensor in the control of the robot, it would be convenient to have the base and shell centre points coincident.

The solution used to make better use of the space and make the two coordinate centres coincide is shown in Fig. 2.5. A standard Gough-Stewart architecture usually consists of 3 pairs of legs. In a pair, both legs usually have a common attachment point on the effector. In the architecture presented, one leg of each pair is flipped on the other side of the attachment point of the effector along the direction of said leg. Following this, the attachment points on the effector of each pair have been moved apart along the frame of the base.

2.6 Geometry and kinetostatics of the mechanism

In order to determine the design parameters of the mechanism, such as the position of the attachment points and the spring stiffness of the elastic passive joints, the kinematic model of the mechanism must be derived.

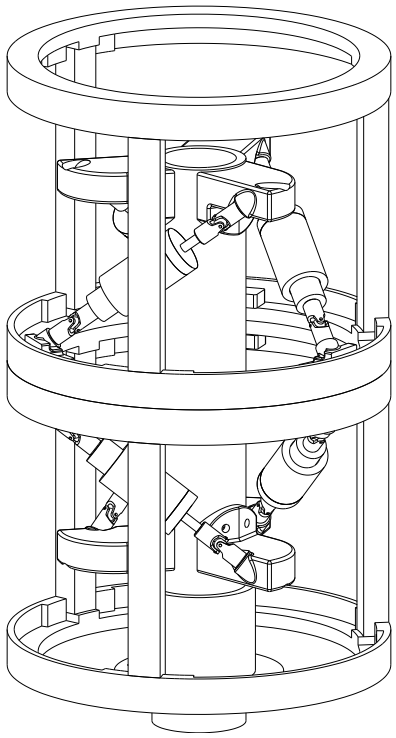

FIGURE 2.5 – Architecture of the 6-dof platform. The center tube is the robot link (base) and the outer skeleton is the support for the shell (effector).

2.6.1 Geometric design

As stated previously, a few design constraints must be taken into account when choosing the parameters of the mechanism. The range of motion of the shell, as well as the passive joints are the first important factors to take into account. In order to find a working architecture, the geometric constraint equations are first needed. In the case of this mechanism, they can be expressed as

$$\rho_i^2 = (\boldsymbol{a}_i - \boldsymbol{b}_i)^T (\boldsymbol{a}_i - \boldsymbol{b}_i) \tag{2.1}$$

where ρ_i is the length of the ith leg, $\boldsymbol{a}_i$ is the position vector of the shell attachment point of the ith leg expressed in the base (link) coordinate frame, and $\boldsymbol{b}_i$ is the position vector of the base attachment point of the ith leg in the base's coordinate frame. The position vector $\boldsymbol{a}_i$ can be expressed as :

$$\boldsymbol{a}_i = \boldsymbol{s} + \boldsymbol{Q}\boldsymbol{a}'_i \tag{2.2}$$

where $\boldsymbol{s}$ is the position vector of the shell's reference point expressed in the base frame, $\boldsymbol{a}'_i$ is the position of the shell attachment point of the ith leg in the shell's coordinate frame, and $\boldsymbol{Q}$ is the rotation matrix corresponding to the orientation of the shell with respect to the base (link). Using these equations, it is possible to compute the leg lengths for any configuration of the shell, for given architectural parameters.

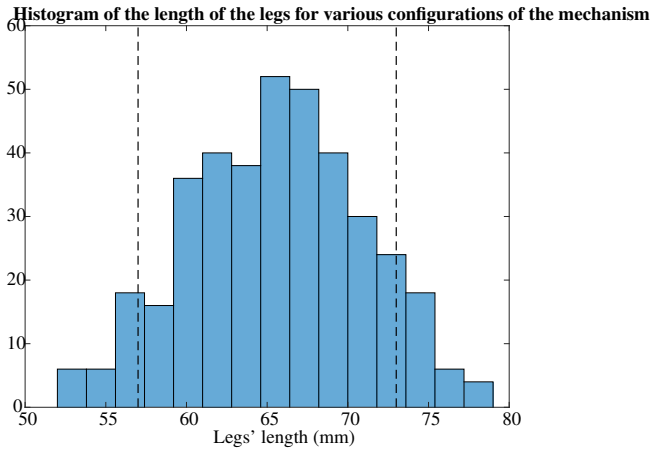

FIGURE 2.6 – Distribution of the length of the legs for the 64 extreme configurations of the mechanism in which each of the 6 Cartesian coordinates is either at its minimum or maximum. The vertical lines represent the mechanical limits of the joints.

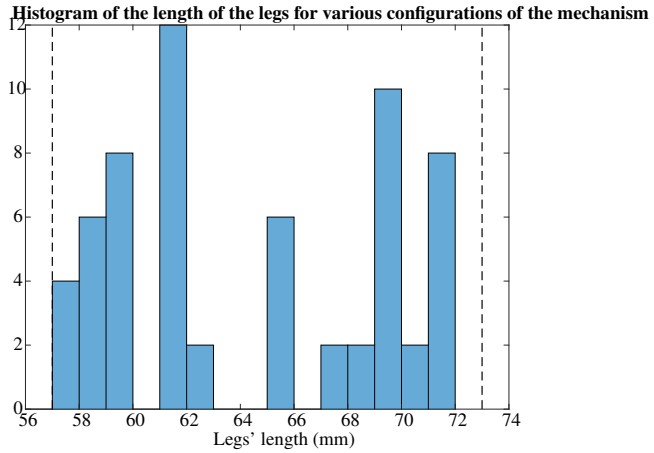

FIGURE 2.7 – Distribution of the length of the legs for 12 pure Cartesian movement configurations of the mechanism in which only one of the 6 Cartesian coordinates was at its minimum or maximum. The vertical lines represent the mechanical limits of the joints.

The position of the attachment points of the mechanism are based on the resting length of the legs. The rest length was determined from mechanical constraints. The rest length must be large enough so that it can contain all the mechanical components such as the spring and the distance sensor, and allow for a range similar to that of the whole mechanism. However, it must also be small enough to keep the parts relatively compact so that they remain light. The resting length chosen was therefore 65 mm.

Figure 2.6 shows the distribution of the length of the legs for the 64 most extreme configurations of the mechanism. These configurations correspond to the vertices of the hypercube describing the workspace of the mechanism in the Cartesian space, i.e., translations of $\pm 1cm$ and rotations of $\pm 10^{\circ}$

around all three axes. These configurations however, are somewhat too extreme to fairly represent the use of the mechanism. One solution is to divide the configuration vector by the square root of the dimension –in our case 6– of the workspace. This roughly represents a hypersphere corresponding to the hypercube of the workspace of the mechanism and is a better representation of the workspace. Figure 2.6 thus represents the extreme configurations on the hypersphere of the workspace. Most of the lengths remain around the mid-range configuration of 65 mm while the most extreme cases show changes of length of around $\pm$12-13 mm.

Figure 2.7 shows the distribution for the points of the workspace located at the centre of the 12 faces of the hypercube of the workspace. These points are obtained by setting one coordinate to its extreme while leaving the others at 0 (centre of the workspace). While this representation of the workspace is far from being a worst-case scenario, it more accurately represents the use of the mechanism. As shown in the figure, with a mid-range configuration of 65 mm, the maximum change of length of the legs is $\pm$ 8 mm. The corresponding limits of the leg lengths are shown as dotted lines in Fig. 2.6 and Fig. 2.7, where it can be observed that most of the extreme configurations are captured using this range of motion of the legs.

2.6.2 Kinematic sensitivity

While it is important that the mechanism can execute all the required movements, it is also important that it remains stable while performing these movements. In order to assess the stability of a mechanism, the kinematic equations of the mechanism are derived. Starting from equation (2.1) and differentiating with respect to time, one has

$$\rho_i \dot{\rho}_i = (\boldsymbol{a}_i - \boldsymbol{b}_i)^T (\dot{\boldsymbol{a}}_i - \dot{\boldsymbol{b}}_i). \tag{2.3}$$

This equation can be simplified since $\dot{\boldsymbol{b}}_i = \boldsymbol{0}$ as $\boldsymbol{b}_i$ is constant. Furthermore, using eq (2.2), $\dot{\boldsymbol{a}}_i$ can be expressed as

$$\dot{\boldsymbol{a}}_i = \dot{\boldsymbol{s}} + \dot{\boldsymbol{Q}}\boldsymbol{a}_i' \tag{2.4}$$

and

$$\dot{\boldsymbol{Q}} = \boldsymbol{\Omega}\boldsymbol{Q} \tag{2.5}$$

with

$$\boldsymbol{\Omega} = \boldsymbol{1} \times \boldsymbol{\omega} \tag{2.6}$$

where $\boldsymbol{1}$ is the identity matrix and $\boldsymbol{\omega}$ is the angular velocity vector of the platform. Equation (2.3) then becomes

$$\rho_i \dot{\rho}_i = (\boldsymbol{a}_i - \boldsymbol{b}_i)^T (\dot{\boldsymbol{s}} + \boldsymbol{\Omega} \boldsymbol{Q} \boldsymbol{a}_i'). \tag{2.7}$$

Using equation (2.6), equation (2.7) can be written as

$$\rho_i \dot{\rho}_i = (\boldsymbol{a}_i - \boldsymbol{b}_i)^T \dot{\boldsymbol{s}} + [(\boldsymbol{Q} \boldsymbol{a}_i') \times (\boldsymbol{a}_i - \boldsymbol{b}_i)]^T \boldsymbol{\omega} \tag{2.8}$$

thereby yielding the relationship between the effector velocity and joint velocity as

$$\boldsymbol{J} \boldsymbol{t} = \boldsymbol{K} \dot{\boldsymbol{\rho}} \tag{2.9}$$

where $\boldsymbol{J}$ and $\boldsymbol{K}$ are the Jacobian matrices, $\dot{\boldsymbol{\rho}}$ is the vector of joint velocities, and $\boldsymbol{t}$ is the vector of the effector velocities and can be expressed as

$$\boldsymbol{t} = \begin{bmatrix} \dot{\boldsymbol{s}}^T & \boldsymbol{\omega}^T \end{bmatrix}^T \tag{2.10}$$

From equation (2.8) it is possible to find the expression of the matrices $\boldsymbol{K}$ and $\boldsymbol{J}$, namely

$$\boldsymbol{K} = \text{diag}[\rho_1, \ldots, \rho_6] \quad \text{and} \quad \boldsymbol{J} = \begin{bmatrix} \boldsymbol{c}_1^T \\ \vdots \\ \boldsymbol{c}_6^T \end{bmatrix} \tag{2.11}$$

with

$$\boldsymbol{c}_i = \begin{bmatrix} (\boldsymbol{a}_i - \boldsymbol{b}_i) \\ (\boldsymbol{Q} \boldsymbol{a}_i') \times (\boldsymbol{a}_i - \boldsymbol{b}_i) \end{bmatrix} \tag{2.12}$$

The Jacobian matrices can be used to assert the quality of the mechanism comfiguration. Indeed, the Jacobian matrices can be used to calculate the kinematic sensitivity index of the mechanism. As stated in [4], the kinematic sensitivity index corresponds to finding a Cartesian displacement $\delta \boldsymbol{x} = [\delta \boldsymbol{s}^T, \delta \boldsymbol{\phi}^T]^T$ which generates a displacement of the joints having a fixed norm $\|\delta \boldsymbol{\rho}\|_2 = 1$ while giving a global extremum for $\|\delta \boldsymbol{\phi}\|_2$ and $\|\delta \boldsymbol{s}\|_2$. For a parallel manipulator the kinematic sensitivity in translation, noted $\boldsymbol{\sigma}_p$, and the kinematic sensitivity in rotation, noted $\boldsymbol{\sigma}_r$, can be defined as

$$\begin{aligned} \sigma_r &\equiv \max_{\|\boldsymbol{K}' \delta \boldsymbol{x}\|_2 = 1} \|\delta \boldsymbol{\phi}\|_2 \\ \sigma_p &\equiv \max_{\|\boldsymbol{K}' \delta \boldsymbol{x}\|_2 = 1} \|\delta \boldsymbol{s}\|_2 \end{aligned} \tag{2.13}$$

where the matrix $\boldsymbol{K}'$ is defined

$$\delta \boldsymbol{\rho} = \boldsymbol{K}' \delta \boldsymbol{x} = \boldsymbol{K}^{-1} \boldsymbol{J} \delta \boldsymbol{x} \tag{2.14}$$

The indices can be computed directly from the Jacobian matrices. The details of the computation of these indices are explained in [4]. For a parallel manipulator such as the displacement sensor proposed here, we can easily compute the inverse kinematics to find the positions $\boldsymbol{a}_i$ and the length of the prismatic joints for a given position and orientation of the platform. An example of the indices for a constant orientation of $\boldsymbol{Q} = \mathbf{1}$ and a constant orientation of $[\phi, \theta, \psi] = [-8, 20, 10]$ for a ZYX Euler angle convention is presented in figure 2.8, which illustrates a typical performance of the mechanism as a movement sensor. These indices represent the ratio of the norm of the movements of the shell over the movements of the prismatic joints. In figure 2.8a, when at the midpoint the ratio is approximately 0.72. This means that for a movement with a magnitude of 1 mm of the joints, the corresponding movement of the shell has a magnitude of 0.72 mm. In the case of the presented mechanism, this means that for a small movement of the shell, the joint movement is relatively large which is a desired behaviour because it makes the acquisition using the distance sensor easier.

The second interesting observation is the variation of the value of the index within the workspace of the mechanism. As previously stated, a smaller value of the index is advantageous for the precision of the mechanism and ideally, the value should remain relatively constant within the workspace of the mechanism in order to keep a uniform precision. As shown in figure 2.8, the variation of the index is very small. Even by imposing a large rotation to the mechanism, the index remains within an acceptable range. The small variation is a sign that the mechanism is indeed stable. When the mechanism is near a singularity (where matrix $\boldsymbol{J}$ becomes singular), the sensitivity increases drastically, which means that the index goes to infinity. Singular configurations occur when a small movement of the effector can be performed without moving the joints, which renders the movement detection impossible. When close to a singularity, the precision of the movement detection deteriorates and can lead to instability in the control of the robot. The sensitivity plots shown here show that the mechanism remains far from singular configurations.

2.6.3 Statics of the mechanism

The mechanism is to be used as a displacement sensor which will be moved by a human user. The mechanism must have the lowest possible impedance so that it is not strenuous for the user [7] to operate and so that the force used to move it is small enough. The force felt by the user is directly related to the force in the springs of the passive prismatic joints [15]. In order for the user force to be low, the spring force must be fairly low so that when a displacement is applied, the joint force is not too large. However, the spring forces must be large enough to maintain the shell close to the mid-range configuration for any orientation of the robot. It is therefore important to find a balance between springs that have a preload that is sufficient to support the shell but weak enough so that the interaction force is not too large. Furthermore when the shell moves, the force must not become too large. This can be accomplished by using springs with a relatively low stiffness and a relatively high pre-load. When moving around the midpoint, the force in the springs is high enough to maintain the mechanism in the mid-range configuration but when moving the shell, the low spring constant prevents the interaction

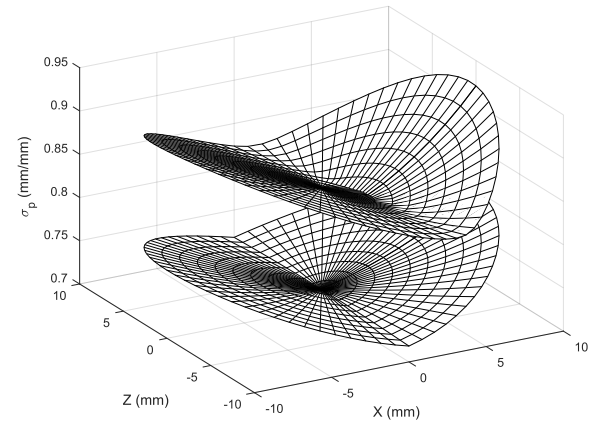

(a)

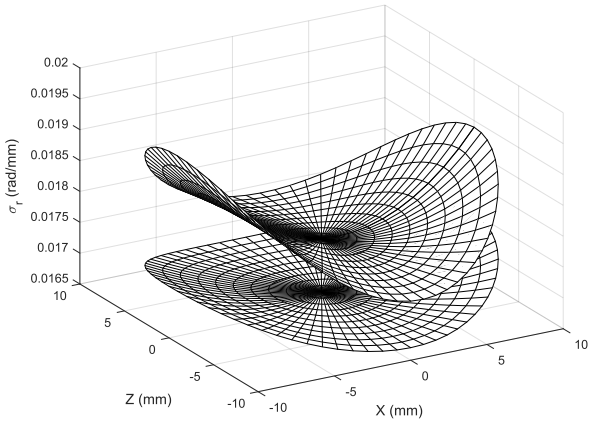

(b)

FIGURE 2.8 – Maximum point-displacement (a) and rotation (b) sensitivity index for a constant orientation $\boldsymbol{Q} = \mathbf{1}$ (bottom surface) and $[\phi, \theta, \psi] = [-8^\circ, 20^\circ, 10^\circ]$ with the ZYX Euler angle convention (top surface).

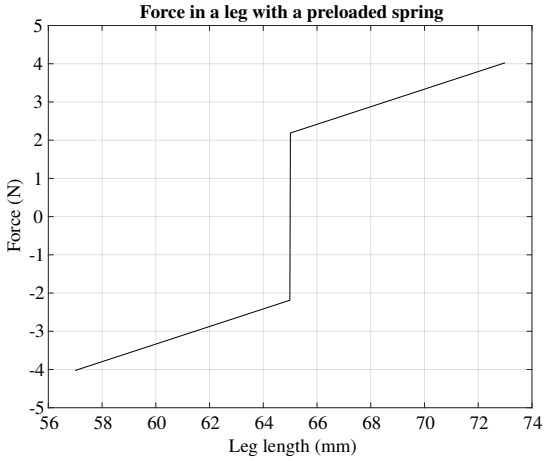

FIGURE 2.9 – Force in the leg as a function of its length. The discontinuity (preload) induces a *dead-band*, i.e., a minimum force is required to make the joint move.

force from becoming too large. The behaviour of the force in the leg is shown in figure 2.9 where the discontinuity corresponds to the preload and the slope corresponds to the stiffness of the spring.

The relationship between the forces at the joints and the forces at the effector, can be found using the principle of virtual work. Indeed, equating the input work at the prismatic joints and the output work at the end-effector, one can write

$$\boldsymbol{f}^T \delta \boldsymbol{x} = \boldsymbol{\tau}^T \delta \boldsymbol{\rho} \tag{2.15}$$

where $\boldsymbol{f}$ is the wrench (force and moment) at the effector, $\delta \boldsymbol{x}$ is a small movement of the effector, $\boldsymbol{\tau}$ is the vector of forces in the prismatic joints, and $\delta \boldsymbol{\rho}$ is a small movement of the prismatic joints.

Substituting equation (2.14) into (2.15) we find

$$\boldsymbol{f}^T \delta \boldsymbol{x} = \boldsymbol{\tau}^T \boldsymbol{K}^{-1} \boldsymbol{J} \delta \boldsymbol{x}. \tag{2.16}$$

Since equation (2.16) must be satisfied for any vector of small displacements $\delta \boldsymbol{x}$, one can write

$$\boldsymbol{f} = \boldsymbol{J}^T \boldsymbol{K}^{-T} \boldsymbol{\tau}. \tag{2.17}$$

Using this relationship, it is possible to find the wrench at the effector by knowing the force at the joints. The forces at the joints are easily computed from the elongation, the stiffness, and the preload of the springs. Using the solution to the inverse kinematics (eq. 2.1), we can impose a movement to the shell and compute the length of the legs. The forces and moments felt by the user are then readily computed using equation (2.17). Since the passive joints use compression springs for both directions of the motion, Hooke's law can simply be applied to find the force in each joint, namely

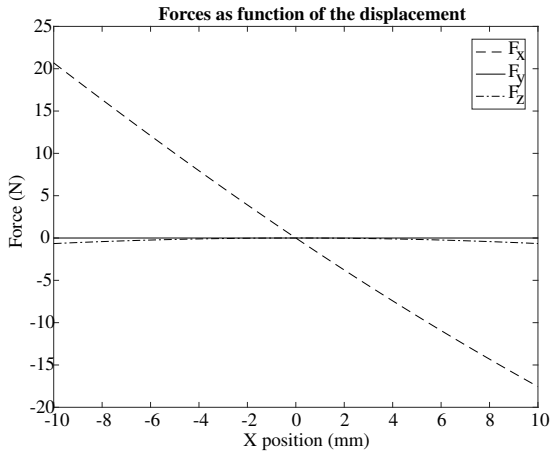

FIGURE 2.10 – Forces along the three axes for a displacement along the x axis of the mechanism.

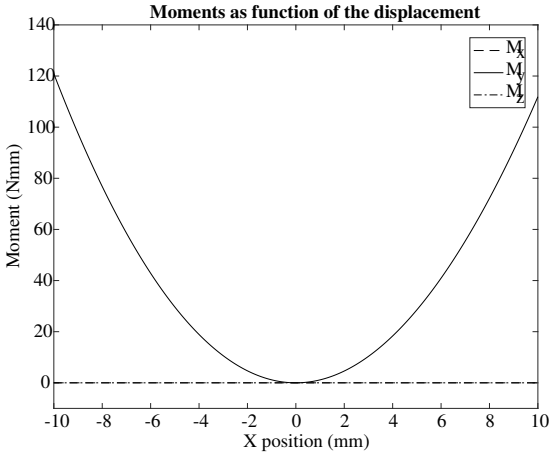

FIGURE 2.11 – Moments along the three axes for a displacement along the x axis of the mechanism. The moments M_x and M_Z are both zero.

$$\tau_i = -sgn(\delta\rho_i)k_i(l_0 + \delta\rho_i) \tag{2.18}$$

where τ_i is the force in the ith prismatic joint, $sgn(\cdot)$ is the signum function, which returns the sign of its argument, k_i is the stiffness of the ith spring, l_0 is the preload compression length, and $\delta\rho_i$ is the change of length of the prismatic joint due to a movement.

With equations (2.17) and (2.18), it is now possible to simulate the movement and find the value of the force and moment at the shell for any configuration.

Examples of the results obtained with such computations are shown in figures 2.10 and 2.11 where the forces and moments along the different axes are plotted for a displacement along the x axis for a spring stiffness of $k = 1$N/mm and no pre-load.

As it can be observed from Figures 2.10 and 2.11, when moving the robot along an axis, some forces and moments can appear along the other axes. This is to be expected since the Jacobian matrix $\boldsymbol{J}$ is not diagonal. Having parasitic forces is an undesirable effect because it directly affects the user experience. When pushing in one direction, facing a reaction force or moment in a different direction is counter-intuitive. It is then important to verify that these parasitic forces and moments are not too large in comparison to the main force in the direction of the movement.

For the displacement presented in figures 2.10 and 2.11, one main parasitic moment can be observed around the y axis, which corresponds to the direction parallel to the longitudinal axis of the robot link. This parasitic moment appears for any displacement or rotation imposed on the shell. It is due to the architecture of the robot, which contains a rotational symmetry. Indeed, the three pairs of legs that go from the base to the shell are all pointing in the same rotational direction. This causes a moment to be induced whenever the shell leaves the neutral configuration.

In order to properly compare the contribution of the parasitic moment to the user feeling to the contribution of the main force, it is better to convert this moment into a tangential force applied on the shell. The shell has a radius of 70mm, therefore a force applied on the shell that is equivalent to the moment produced by the joints would be of approximately 1.7N when the shell is moved to the -10mm position. The force along the x axis for this position is approximately 20N, which is more than 10 times larger than the force due to the parasitic moment. Therefore, the parasitic moment around the y axis can be considered negligible especially when taking into account that the shell should almost never reach this extreme point. Indeed, when the sensor is in use, the robot is trying to follow the sensor as closely as possible which means that, with proper control, the shell should stay relatively close to the neutral mid-range configuration. As an example, for a movement of 2mm, the force is approximately 4N and the moment is approximately 4.5Nmm. When transformed into a force on the shell, the moment is equivalent to a force of 0.0065N which is more than 60 times smaller than the main force. These forces are therefore negligible and will not significantly affect the user feeling, even in the most extreme cases.

The rotational symmetry does not only induce parasitic moments but it also makes force along one axis not symmetric between the positive and negative directions. As it can be observed in figure 2.10, the force along the x axis is larger when moving in the negative direction than when moving in the positive direction. This effect is especially visible when considering the extrema of the movement where there is a difference of approximately 3 to 4N. Such differences are an undesired behaviour because they are not intuitive. However, these effects are much less significant around the mid-range configuration. Furthermore, using the preload and lower spring stiffness, these effects can be mitigated.

The effect of adding a preload is shown in figure 2.9. The preload induces a discontinuity in the force when moving through the mid-range configuration. This means that a minimum force has to be applied in order to move the shell. This is essential in order to alleviate the effect of gravity on the mechanism. Since the shell has a mass, gravity will apply a force on it and can potentially move the shell. Since

the shell is used as a control input device, gravity must not influence the position of the shell. In [18], the mechanism must also support the payload's weight, but has the advantage of not having to deal with orientation changes. Furthermore, counterweights were used in [18] to balance the weight of the payload and mechanism because only translations were performed. For the mechanism presented here, orientation changes make it challenging to balance the mechanism using counterweights or springs. Instead, the preload of the joints is used to compensate for gravity. With a proper adjustment of the preload forces, the shell force threshold can be high enough so that the weight and inertia of the shell itself are not large enough to allow movement of the shell for any orientation or movement of the robot.

With a proper preload, it is possible to use a low spring stiffness to give the user a smooth feeling. Ideally, once the mechanism is displaced from its mid-range configuration, the reaction force should remain as constant as possible during the whole movement, which can be accomplished by using a low spring stiffness. This parameter can be used to tune the user feeling and find a setting for which the mechanism is stiff enough to offer a good feeling while not being too difficult to move for the user.

2.7 Prototype and Tests

With the design parameters well established, a prototype is then built and tested.

2.7.1 Passive Joints and Mechanism

The passive prismatic joints of the prototype are made of ABS plastic using a 3D printing machine for the housing, shaft and floating parts. The passive universal joints are off-the-shelf components. The springs are steel springs with a selected stiffness and cut to the appropriate length to obtain a chosen preload force.

A thin plexiglass sheet supported by ABS rings is used for the shell. A photograph of the mechanism is shown in figure 2.12.

2.7.2 Forward Kinematics

While the whole design phase could be completed using only the inverse kinematics, the actual use of the sensor requires to calculate the position and orientation of the shell using the length of the legs of the mechanism. As mentioned above, while the inverse kinematics of a parallel mechanism are often very simple, the forward kinematics can be challenging. The direct kinematics of the Gough-Stewart platform yields a very complex 40th degree polynomial equation [12]. It is even possible in some cases to find architectures with 40 real solutions [9]. Although some algorithms exist to solve the 40th degree polynomial equation [13], it is not the most practical method for our application. Luckily, the Gough-Stewart platform is one of the most studied parallel mechanisms and multiple numerical techniques [6] can be employed to solve the forward kinematics.

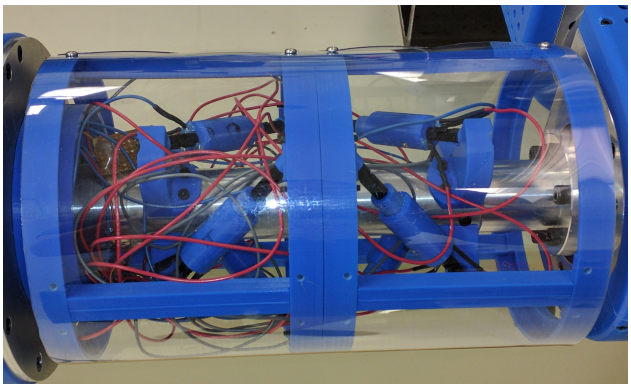

FIGURE 2.12 – Prototype of the 6-dof low-impedance elastic displacement sensor. The robot link and the prismatic legs are visible inside the transparent shell.

One common and simple numerical method used to solve the forward kinematics is to use the Newton-Raphson algorithm. This relatively simple algorithm requires a first approximation of the solution $\boldsymbol{x}_i$, then converges to the zero of a goal function $\boldsymbol{f}(\boldsymbol{x},\boldsymbol{\rho})$ by iterating over the value of $\boldsymbol{x}$. The vector $\boldsymbol{x}$ can be expressed as

$$\boldsymbol{x} = \begin{bmatrix} \boldsymbol{s}^T & \boldsymbol{\phi}^T \end{bmatrix}^T \tag{2.19}$$

where $\boldsymbol{s}$ is the position vector of the reference point of the shell and $\boldsymbol{\phi}$ is the array containing the three Euler angles used to represent the rotation of the shell with the *ZYX* convention. Euler angles are simple to use but suffer from a major drawback. Depending on the convention used, formulation singularities can be present for some given rotations. The *ZYX* convention however is stable around the $(0,0,0)$ orientation and the singularities lay outside of the mechanism's range of motion which makes the use of this convention of Euler angles suitable.

While this method is relatively simple and robust, the initial guess must be relatively close to the solution.

While in use, the mechanism senses a movement which is used to control a serial robot. In this application, the robot actually tries to follow the movement of the sensor as closely as possible and as fast as possible. This means that even though the mechanism has a relatively large range of motion, most of the time it will remain close to its mid-range configuration. This is a great advantage when using the Newton-Raphson algorithm since the initial guess will almost always be very close to the actual solution. With that being known and based on equation (2.1), we can express the goal function as

$$f_i^2 = (\boldsymbol{a}_i - \boldsymbol{b}_i)^T (\boldsymbol{a}_i - \boldsymbol{b}_i) - \rho_i^2. \tag{2.20}$$

$$\boldsymbol{g} = \begin{bmatrix} f_1^2 & f_2^2 & \dots & f_n^2 \end{bmatrix}^T \tag{2.21}$$

For a given initial guess $\boldsymbol{x}_0$, function $\boldsymbol{g}$ can be computed. A limited Taylor expansion around the initial guess can then be used to find the next estimate of the solution as the solution of the following linear system

$$\frac{\partial \boldsymbol{g}}{\partial \boldsymbol{x}} \delta \boldsymbol{x} = -\boldsymbol{g}(\boldsymbol{x}_0) \tag{2.22}$$

The next estimate is then computed as

$$\boldsymbol{x}_i = \boldsymbol{x}_0 + \delta \boldsymbol{x} \tag{2.23}$$

This procedure is repeated until the magnitude of the vector $\boldsymbol{g}$ is smaller than a predefined threshold. It is noted that matrix $\frac{\partial \mathbf{g}}{\partial \mathbf{x}}$ is almost identical to the Jacobian matrix $\boldsymbol{J}$ defined in equation (2.12) except that one has

$$\boldsymbol{c}_i = \begin{bmatrix} (\boldsymbol{a}_i - \boldsymbol{b}_i) \\ ((\boldsymbol{Q}\boldsymbol{a}_i') \times (\boldsymbol{a}_i - \boldsymbol{b}_i))^T \boldsymbol{S} \end{bmatrix} \tag{2.24}$$

where $\boldsymbol{S}$ is a matrix defined according to the Euler angle convention used [1].

2.7.3 Tests

The mechanism described in this paper is mounted on the last link of a five-degree-of-freedom custom serial robot shown in figure 2.13. Based on the control scheme presented in [17], a control algorithm was developed which uses the displacement measured by the mechanism to move the robot. Tests were conducted in which the displacement of the sensor is measured and the effector is moved in the direction of the movement. Using the data from the position sensors in the sensing mechanism and the encoders of the robot, the position of the shell of the mechanism and the position of the effector of the robot are computed.

Figures 2.14–2.16 show the position of the effector and low-impedance mechanism along the 3 Cartesian axes while figure 17 shows the results for oscillating motions along the X axis. The figures show that the effector can follow the sensor closely. The control algorithm uses the direction measured by the sensor as an input. The results shown in the figures indicate that the displacement measurement is accurate.

Figure 2.17 shows an oscillating movement performed using the sensing mechanism. The stability of the mechanism and its bandwidth are very important in order for the human user to feel safe. As shown in the figure, the robot can follow the sensor closely for an oscillating movement. It is important to note that, for higher frequencies, the amplitude must be lower for the robot to be able to follow.

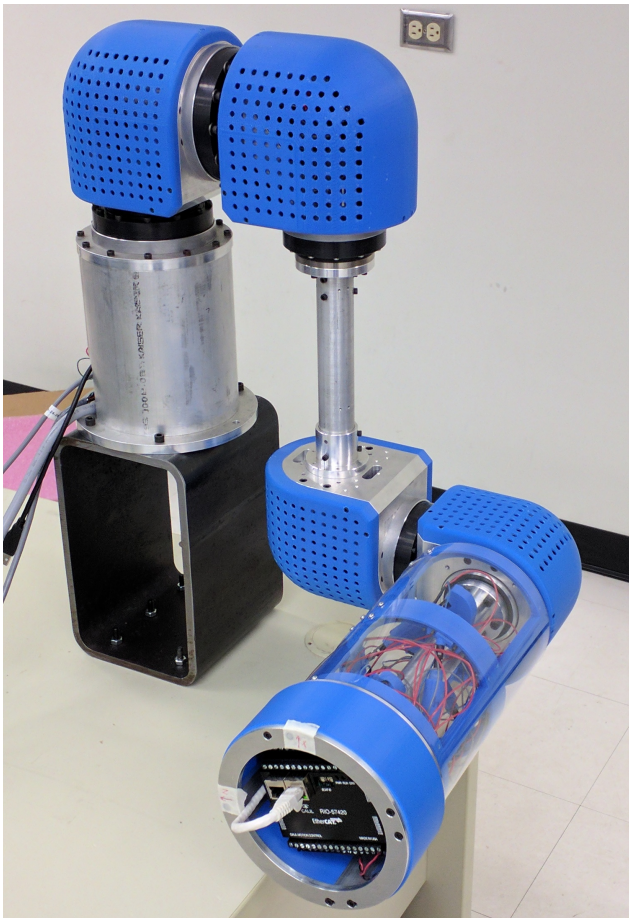

FIGURE 2.13 – 5-dof robot with the 6-dof displacement sensing mechanism mounted at the effector.

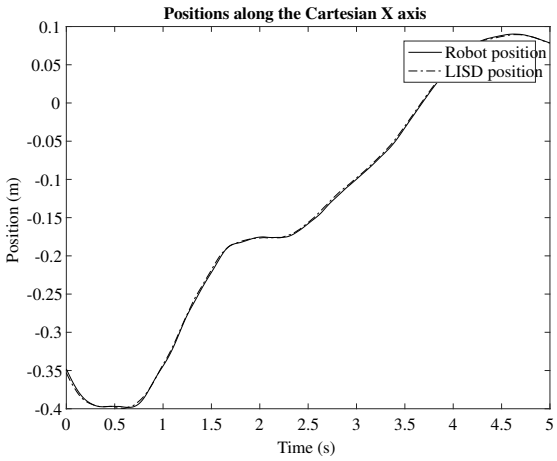

FIGURE 2.14 – Position along the X axis of the global coordinate system.

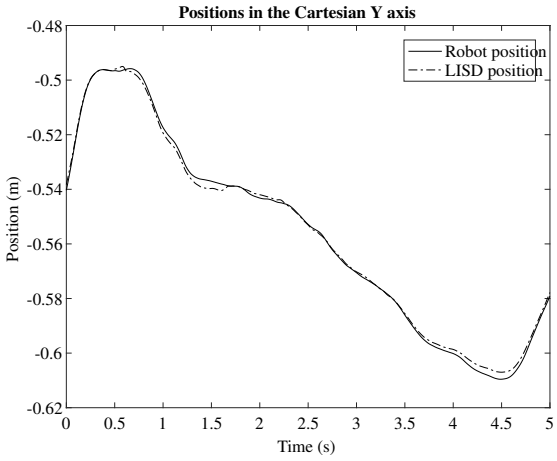

FIGURE 2.15 – Position along the Y axis of the global coordinate system.

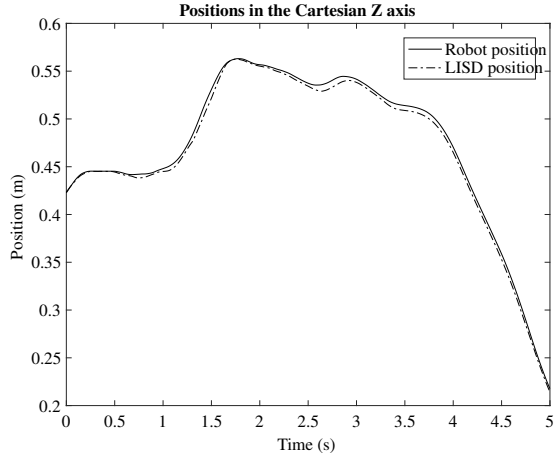

FIGURE 2.16 – Position along the Z axis of the global coordinate system.

2.8 Conclusion

The mechanical design of a low-impedance displacement sensor for intuitive human-robot interaction was presented in this article. The general approach was presented and the advantages of the passive elastic parallel mechanism were explained. The design of the passive elastic joints were then detailed as well as the overall architecture of the sensing mechanism, which is based on the Gough-Stewart platform. Next, the geometric design of the sensing mechanism as well as an analysis of its kinematic sensitivity and statics were presented. These two properties are the most important when dealing with position sensing in a human-robot interaction context. Finally a prototype of the 6-dof sensing mechanism was presented which was then tested with a 5-dof serial robot. The sensor was able to measure the proper movements in order to control the custom 5-dof robotic arm. Future work includes different versions of the low-impedance sensing device, more notably a 3-dof version that allow only

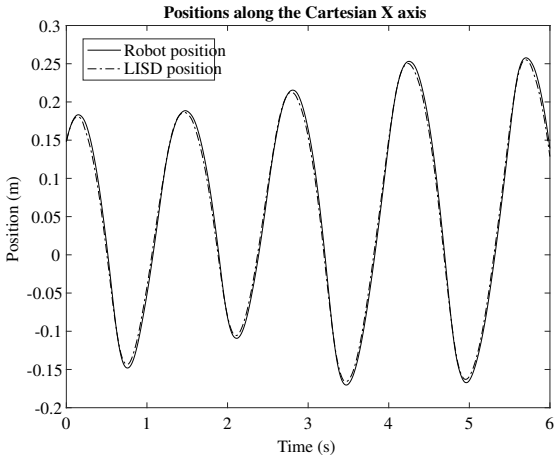

FIGURE 2.17 – Oscillating movement of the sensor and robot along the X cartesian axis.

translations.

2.9 Acknowledgements

The authors would like to acknowledge the financial support of the Natural Sciences and Engineering Research Council of Canada (NSERC) and of the Canada Research Chair program.

Conclusion

L'approche présentée dans ce mémoire se veut tout d'abord une preuve de concept pour une nouvelle méthode de contrôle de bras robotiques sécuritaire et intuitive. Cette approche permet à un utilisateur humain de déplacer un bras robotique de façon complètement intuitive permettant ainsi à un utilisateur complètement étranger au système d'utiliser le robot facilement. Par contre, le prototype ayant seulement 5 degrés de liberté ne permet pas de tester au maximum les capacités de l'algorithme. Ce nombre de degrés de liberté est assez grand pour donner l'impression à l'utilisateur que tous les mouvements sont possibles tout en restant plutôt contraignant.

Le développement d'un capteur de mouvement permet non seulement de rendre possible cette méthode de contrôle sur un bras robotique, mais aussi de la rendre sécuritaire. En effet, l'utilisateur n'entre jamais en contact direct avec le bras robotique car ses intentions sont déduites à l'aide d'une interface passive élastique. Bien entendu, le système n'est pas conçu afin d'exécuter une tâche particulière mais bien afin de simplement déplacer le robot dans son espace de travail. La méthode reste très performante et intuitive lorsque le robot n'interagit pas avec l'environement mais lorsque ce dernier doit effectuer des tâches qui nécessitent un contact avec l'environement certains problèmes peuvent potentiellement survenir. De plus, les joints du capteur doivent quand même supporter le poids de ce dernier et la précontrainte doit demeurer relativement grande et ainsi affecter la sensation de l'utilisateur.

Les objectif de ce projet ont tout de même été atteints et la méthode est non seulement fonctionnelle, mais aussi plus performante qu'un robot collaboratif commercial.

Travaux futurs

Les fondations ont étés établies afin de continuer à travailler à l'amélioration de l'approche macro-mini pour les bras robotiques sériels. Voici certaines avenues qui peuvent êtres explorées :

Tout d'abord au niveau de l'architecture du capteur, les possibilités sont presques infinies. La plateforme de Gough-Stewart offre un bon point de départ pour démontrer le fonctionnement du concept, mais les architectures parallèles sont extrèmement variées et méritent d'être explorées.

Les mécanismes compliants peuvent offrir une bonne alternative au mécanisme présenté ici afin de

réduire le nombre de pièces mobiles dans le système.

Pour les membrures plus près de la base, des capteurs de mouvement ayant moins de degrés de liberté peuvent s'avérer plus intuitifs que le capteur ayant 6 degrés de liberté. Ceci offre aussi la possibilité d'utiliser des mécanisme équilibrés et ainsi réduire la précontrainte nécessaire dans les joints et améliorer la sensation de l'utilisateur.

Au niveau du contrôle, l'algorithme présenté doit être optimisé et retravaillé. Au niveau de l'approche générale, une grande variété de méthodes de contrôle différentes peuvent être explorées. En effet, plusieurs capteurs de mouvement peuvent être utilisés en même temps et l'interaction de ceux-ci peut être explorée. Il sera aussi intéressant de voir le capteur à 6 degrés de liberté à l'oeuvre sur un robot ayant 6 ou même 7 degrés de liberté.

Ensuite, avec des capteurs aux différentes membrures et un robot ayant au moins 7 degrés de liberté, l'idée de la redondance peut aussi être explorée.

Finalement, afin de remédier aux problèmes rencontrés lors de l'interaction avec l'environnement, l'utilisation d'un capteur d'effort à l'effecteur et son intégration dans la boucle de contrôle pourraient être une piste intéressante à explorer.

Bibliographie

[1] Jorge ANGELES et J ANGELES : *Fundamentals of robotic mechanical systems*, volume 2. Springer, 2002.

[2] Nicolas BADEAU, Clément GOSSELIN, Simon FOUCAULT, Thierry LALIBERTÉ et Muhammad E ABDALLAH : Intuitive physical human–robot interaction. *IEEE Robotics & Automation Magazine*, 1070(9932/18), 2018.

[3] Fethi BELKHOUCHE : An optimal time strategy for collision avoidance between collaborative agents. *In American Control Conference (ACC), 2017*, pages 1328–1333. IEEE, 2017.

[4] Philippe CARDOU, Samuel BOUCHARD et Clément GOSSELIN : Kinematic-sensitivity indices for dimensionally nonhomogeneous jacobian matrices. *IEEE Transactions on Robotics*, 26(1): 166–173, 2010.

[5] Andrea CHERUBINI, Robin PASSAMA, André CROSNIER, Antoine LASNIER et Philippe FRAISSE : Collaborative manufacturing with physical human–robot interaction. *Robotics and Computer-Integrated Manufacturing*, 40:1–13, 2016.

[6] Bhaskar DASGUPTA et TS MRUTHYUNJAYA : The Stewart platform manipulator : a review. *Mechanism and machine theory*, 35(1):15–40, 2000.

[7] Agostino DE SANTIS, Bruno SICILIANO, Alessandro DE LUCA et Antonio BICCHI : An atlas of physical human–robot interaction. *Mechanism and Machine Theory*, 43(3):253–270, 2008.

[8] Arati S DEO et Ian D WALKER : Overview of damped least-squares methods for inverse kinematics of robot manipulators. *Journal of Intelligent and Robotic Systems*, 14(1):43–68, 1995.

[9] Peter DIETMAIER : The Stewart-Gough platform of general geometry can have 40 real postures. *In Advances in Robot Kinematics : Analysis and Control*, pages 7–16. Springer, 1998.

[10] G GRUNWALD, G SCHREIBER, A ALBU-SCHAFFER et G HIRZINGER : Touch : The direct type of human interaction with a redundant service robot. *In Robot and Human Interactive Communication, 2001. Proceedings. 10th IEEE International Workshop on*, pages 347–352. IEEE, 2001.

[11] Sami HADDADIN, Alin ALBU-SCHÄFFER et Gerd HIRZINGER : Requirements for safe robots : Measurements, analysis and new insights. *The International Journal of Robotics Research*, 28(11-12):1507–1527, 2009.

[12] Manfred L HUSTY : An algorithm for solving the direct kinematic of Stewart-Gough-type platforms. *Mechanism and Machine Theory*, 31(4):365–380, 1996.

[13] Carlo INNOCENTI : Forward kinematics in polynomial form of the general Stewart platform. *Journal of Mechanical Design*, 123(2):254–260, 2001.

[14] Oussama KHATIB : Augmented object and reduced effective inertia in robot systems. *In American Control Conference, 1988*, pages 2140–2147. IEEE, 1988.

[15] Kazuhiro KOSUGE, Minoru OKUDA, Toshio FUKUDA, T KODUKA et Tatsuya MIZUNO : Input/output force analysis of Stewart platform type of manipulators. *In Intelligent Robots and Systems' 93, IROS'93. Proceedings of the 1993 IEEE/RSJ International Conference on*, volume 3, pages 1666–1673. IEEE, 1993.

[16] Jörg KRÜGER, Terje K LIEN et Alexander VERL : Cooperation of human and machines in assembly lines. *CIRP Annals-Manufacturing Technology*, 58(2):628–646, 2009.

[17] Pascal D LABRECQUE, Jacques-Michel HACHÉ, Muhammad ABDALLAH et Clément GOSSELIN : Low-impedance physical human-robot interaction using an active–passive dynamics decoupling. *IEEE Robotics and Automation Letters*, 1(2):938–945, 2016.

[18] Pascal D LABRECQUE, Thierry LALIBERTÉ, Simon FOUCAULT, Muhammad E ABDALLAH et Clément GOSSELIN : uMan : A low-impedance manipulator for human–robot cooperation based on underactuated redundancy. *IEEE/ASME Transactions on Mechatronics*, 22(3):1401–1411, 2017.

[19] Nicolas LAUZIER, Martin GRENIER et Clément GOSSELIN : 2 dof cartesian force limiting device for safe physical human-robot interaction. *In Robotics and Automation, 2009. ICRA'09. IEEE International Conference on*, pages 253–258. IEEE, 2009.

[20] Alexandre LECOURS, Boris Mayer ST-ONGE et Clément GOSSELIN : Variable admittance control of a four-degree-of-freedom intelligent assist device. *In Proc. IEEE Int. Conf. Robot. Autom.*, pages 3903–3908, 2012.

[21] R NAIR et John H MADDOCKS : On the forward kinematics of parallel manipulators. *The International Journal of Robotics Research*, 13(2):171–188, 1994.

[22] Prabjot NANUA, Kenneth J WALDRON et Vasudeva MURTHY : Direct kinematic solution of a Stewart platform. *IEEE transactions on Robotics and Automation*, 6(4):438–444, 1990.

[23] Gennaro RAIOLA, Carlos Alberto CARDENAS, Tadele Shiferaw TADELE, Theo de VRIES et Stefano STRAMIGIOLI : Development of a safety-and energy-aware impedance controller for collaborative robots. *IEEE Robotics and Automation Letters*, 3(2):1237–1244, 2018.

[24] Andre SHARON, Neville HOGAN et David E HARDT : High bandwidth force regulation and inertia reduction using a macro/micro manipulator system. *In Robotics and Automation, 1988. Proceedings., 1988 IEEE International Conference on*, pages 126–132. IEEE, 1988.

[25] S-M SONG *et al.* : Forward kinematics of a class of parallel (Stewart) platforms with closed-form solutions. *In Robotics and Automation, 1991. Proceedings., 1991 IEEE International Conference on*, pages 2676–2681. IEEE, 1991.

[26] Doug STEWART : A platform with six degrees of freedom. *Proceedings of the Institution of Mechanical Engineers*, 180(1):371–386, 1965.

[27] Tadele Shiferaw TADELE, Theo de VRIES et Stefano STRAMIGIOLI : The safety of domestic robotics : A survey of various safety-related publications. *IEEE Robotics & Automation Magazine*, 21(3):134–142, 2014.

[28] Richard Q van der LINDE et Pien LAMMERTSE : Hapticmaster–a generic force controlled robot for human interaction. *Industrial Robot : An International Journal*, 30(6):515–524, 2003.